DEVELOPMENTAL NEUROSCIENCE

Axodendritic versus axosomatic cochlear efferent termination is determined by afferent type in a hierarchical logic of circuit formation

Jemma L. Webber[1], John C. Clancy[1], Yingjie Zhou[1], Natalia Yraola[1], Kazuaki Homma[2,3], Jaime García-Añoveros[1,3,4]*

Hearing involves a stereotyped neural network communicating cochlea and brain. How this sensorineural circuit assembles is largely unknown. The cochlea houses two types of mechanosensory hair cells differing in function (sound transmission versus amplification) and location (inner versus outer compartments). Inner (IHCs) and outer hair cells (OHCs) are each innervated by a distinct pair of afferent and efferent neurons: IHCs are contacted by type I afferents receiving axodendritic efferent contacts; OHCs are contacted by type II afferents and axosomatically terminating efferents. Using an *Insm1* mouse mutant with IHCs in the position of OHCs, we discover a hierarchical sequence of instructions in which first IHCs attract, and OHCs repel, type I afferents; second, type II afferents innervate hair cells not contacted by type I afferents; and last, afferent fiber type determines if and how efferents innervate, whether axodendritically on the afferent, axosomatically on the hair cell, or not at all.

INTRODUCTION

The mammalian cochlear sensory epithelium, the organ of Corti, has two types of mechanosensory hair cells, each innervated by a distinct type of afferent and efferent neuron (*1*). Together, these sensorineural components form a circuit that subserves the sense of hearing. Inner hair cells (IHCs) are arranged in a single row extending along the length of the cochlea and situated in the medial (also termed neural) portion of the organ of Corti, which we refer to as the inner compartment. Outer hair cells (OHCs) are arranged in three rows situated in the lateral (or abneural) region of the organ of Corti, which we refer to as the outer compartment. IHCs and OHCs differ in both morphology and function, with IHCs transmitting the bulk of sensory input to the brain and OHCs fine-tuning and amplifying the incoming auditory signals (*2*–*5*). This dichotomy is also evidenced by the distinct environments that surround the IHCs and OHCs, with unique types of supporting cells [inner border cells (IBCs), inner phalangeal cells (IPhCs), and inner pillar cells (IPCs) versus outer pillar cells (OPCs), Deiters' cells (DCs), and Hensen's cells) housed within the inner or outer compartment (Fig. 1A) (*6*–*8*), as well as by the differential afferent and efferent innervation.

Afferent innervation relays information from the cochlea to the central auditory system, via two types of neurons that reside in the cochlear spiral ganglion. Type I afferents, which comprise most of the spiral ganglion neurons (SGNs), send out processes that each directly synapse onto a single IHC (*9*). Each IHC, in turn, is contacted by 10 to 20 type I afferents, each of which form specialized ribbon synapses, in which a presynaptic ribbon, surrounded by glutamate-filled vesicles in an IHC, apposes a postsynaptic type I afferent nerve ending endowed with glutamate receptors (GluR2/3) (*10*). Type II afferents, which comprise ~5% of the SGNs, send processes that do not form synapses with the IHCs and instead bypass them to enter the outer compartment (*11*). Once in the outer compartment, type II fibers turn toward the base of the cochlea and extend under the OHCs, with which they contact by projecting short, thin collaterals, so that each type II afferent innervates multiple OHCs (Fig. 1B).

Two types of efferent fibers provide descending information from the central auditory system to modulate hair cell and afferent neuronal activity. These efferent neurons originate in the lateral versus medial superior olive (LSO or MSO, respectively) of the brainstem and project into the cochlear organ of Corti (*12*). The lateral olivocochlear (LOC) efferents innervate the inner compartment but do not synapse onto the IHCs. Instead, LOC terminals form axodendritic synapses with the numerous type I afferent fibers innervating the IHCs (Fig. 1B) (*13*). In the mature cochlea, medial olivocochlear (MOC) efferents project into the outer compartment and form direct axosomatic synapses with the OHCs, in close association with the boutons of the type II afferents (Fig. 1B) (*14*). This intricate circuit is reiterated along the length of the organ or Corti. Functionally, the IHC to type I afferent synapses transmit the bulk of the auditory information to the brain, while the OHCs primary role is amplification, with the efferents providing feedback and modulating the response to noise (*15*, *16*). We know little, however, about how this sensorineural circuit is developmentally assembled.

In mouse, cochlear hair cell progenitors exit the cell cycle around E12.5 (embryonic day 12.5) to E14.5 in an apical to basal gradient along the length of the cochlea (*17*, *18*), and nascent hair cells begin to differentiate, in the reverse direction, starting at the base ~E14.5 (*19*). SGNs extend projections toward the developing cochlear epithelium before hair cell differentiation (~E12.5), but they halt at the edge of the spiral lamina and only begin to contact IHCs as they differentiate (*20*, *21*). Thus, in the base of the cochlea, type I afferents contact the IHCs in the inner compartment around E14.5, while type II afferents are first unambiguously detected in the outer compartment ~E18.5 (*20*, *22*–*24*). By birth, the differential innervation

[1]Department of Anesthesiology, Feinberg School of Medicine, Northwestern University, Chicago, IL 60611, USA. [2]Department of Otolaryngology–Head and Neck Surgery, Feinberg School of Medicine, Northwestern University, Chicago, IL 60611, USA. [3]The Hugh Knowles Center for Clinical and Basic Science in Hearing and its Disorders, Northwestern University, Chicago, IL 60611, USA. [4]Departments of Neurology and Physiology, Feinberg School of Medicine, Northwestern University, Chicago, IL 60611, USA.
*Corresponding author. Email: anoveros@northwestern.edu

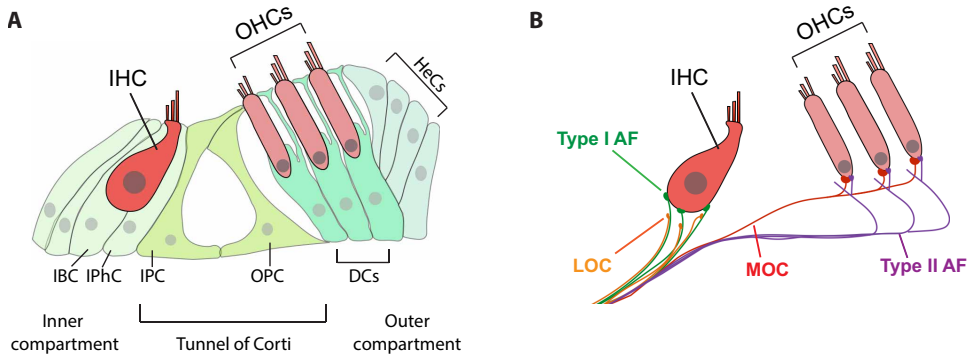

Fig. 1. Structural organization of the organ of Corti. (**A**) The organ of Corti has a row of IHCs and three rows of OHCs surrounded by distinct types of supporting cells. IBCs and IPhCs surround IHCs in the inner compartment. Three rows of DCs underlie OHCs in the outer compartment. Compartments are separated by a single row of IPCs and OPCs that, in the mature cochlea, form a tunnel of Corti. Hensen's cells (HeCs) flank the outer compartment. (**B**) The mature organ of Corti is innervated by two types of afferents (type I and type II) and two types of efferents (MOCs and LOCs). Type I afferents (green) make single connections with IHCs, while type II afferents (purple) cross into the outer compartment, turn basally, and send collateral projections to multiple OHCs. MOCs and LOCs also terminate differentially, with LOCs (orange) making axodendritic contact with type I afferents underneath the IHCs and MOCs (red) forming axosomatic contact with OHCs, in close contact with type II afferents.

of IHCs by radial type I afferents and of the outer compartment by "spiraling" type II afferents beneath the OHCs has been established (*23*, *25*). However, the type II collateral extensions that contact the OHCs are not apparent until around postnatal day 8 (P8) (*26*–*28*).

At least two antagonistic signaling cues operate in the outer compartment early in development to prevent its innervation by type I afferents: (i) OHCs express the membrane-bound repulsive ligand ephrin-A5, whose receptor, Eph4, is expressed by type I afferents (*29*); and (ii) OHCs and other cells in the outer compartment also express the secreted chemorepellent Semaphorin 3F, which acts through the neuropilin 2 receptor on the neurons to prevent type I afferent neurite extension (*23*). In contrast, little is currently known about what guides type II afferents. Supporting cells ensure that type II fibers turn correctly toward the base upon entering the outer compartment (*30*–*33*). However, it is unclear why type II afferents pass by IHCs but fail to innervate them. It has been hypothesized that type I fibers innervating the IHCs outcompete type II afferents arriving subsequently and thus prevent their innervation of IHCs (*29*, *34*). To date, however, an experimental model to test whether type II afferents could innervate IHCs in the absence of type I afferent innervation has not been available.

Efferent fibers arrive to the organ of Corti a few days after the afferents. In mice, choline acetyltransferase or the vesicular acetylcholine transporter (vAChT) labeled MOC fibers/terminals, appear underneath the IHCs by ~P3, and begin to extend into the outer compartment by ~P6 (*13*, *24*, *35*). Consistently, ultrastructural studies show the first axosomatic contacts between MOC fibers and IHCs or OHCs at ~P3 and ~P9, respectively (*13*, *36*). However, the MOC fiber contact with the IHCs is transient and eliminated by P12 (*13*, *37*). LOC fibers arrive at the inner compartment after the MOC fibers but do not innervate the IHCs. Instead, LOC fibers establish axodendritic contacts with the type I afferents that innervate the IHCs (*13*, *15*, *38*). Some evidence indicates that afferents guide efferents into the cochlea, because in the absence of afferents, the efferents fail to reach it (*13*, *39*). However, we remain ignorant of what guides efferent navigation once in the cochlea. Furthermore, it is entirely unknown why LOC efferent fibers innervating the inner compartment terminate axodendritically on the afferents, whereas MOC fibers innervating the outer compartment synapse axosomatically onto the hair cells.

In *Insm1* mutant mice, IHCs are found in the outer compartment, amidst OHCs (*40*). INSM1 is a zinc finger transcription factor that is transiently expressed in nascent OHCs (~E15.5 at the base to P2 at the apex) (*41*). In the absence of INSM1, either in complete or conditional knockouts, immature OHCs are generated in the outer compartment and initially express the earliest markers that characterize them. However, within 1 or 2 days, around half of the nascent OHCs switch fate, transdifferentiating into IHCs. This is evident by the loss of early OHC markers such as BCL11B and the expression of early IHC markers such as *fgf8* mRNA (*40*). As development proceeds, transformed cells maintain an IHC fate, displaying all known mature IHC features including the following: stereocilia size and arrangement, cell shape, nuclear size, expression of numerous protein and mRNA markers, and lack of electromotility (table S1). We conclude that these cells, which we term outer compartment IHCs (oc-IHCs), are mature IHCs in the position of OHCs.

Transdifferentiation of nascent OHCs into IHCs is completed several days before innervation of the outer compartment, i.e., synaptic contact of type II fibers with the OHCs and arrival of efferent fibers both occur after birth. Thus, *Insm1* mutants represent an experimental model with which to determine whether the differential afferent and efferent innervation of IHCs and OHCs is due to the hair cell properties or location within the inner or outer compartment. Here, we find that type I afferents cross into the outer compartment to innervate oc-IHCs, except when encountering an interposed OHC; that type II afferents in the outer compartment innervate oc-IHCs only if they are not innervated by type I afferents; and that the type of afferent fiber that a cell receives then determines if and how efferent fibers will terminate, whether axodendritically on type I afferent fibers, axosomatically on the hair cells, or not at all. Together, our findings reveal a hierarchical logic for development of cochlear innervation: (i) IHCs attract, and OHCs repel, innervation by type I afferents; (ii) type II afferents innervate the remaining HCs, which in normal conditions are OHCs; and (iii) efferent termination is then determined not by the type of hair cell or by its location but by the type of innervating afferent a hair cell receives.

RESULTS

Transdifferentiated oc-IHCs are surrounded by supporting cell types of the outer, and not the inner, compartment

We conditionally ablated *Insm1* using *Atoh1-Cre* (*17*), which is expressed around E13.5 in cochlear and supporting cells, before the onset of *Insm1* expression. As previously reported (*40*), we observe a transformation of around half of all OHCs into IHCs. These oc-IHCs appear to be, but for their ectopic location, otherwise normal IHCs, displaying multiple IHC characteristics [including nuclear size, stereocilia shape, and numerous protein and mRNA markers described previously (*40*) and here (table S1 and fig. S1)]. Physiologically, oc-IHCs display the IHC-characteristic Ik,f (BK-mediated) instead of the KCNQ4-mediated currents characteristic of OHCs, are not electromotile (a feature of OHCs but not IHCs), yet do mechanotransduce (evidenced from their uptake of FM1-43), as expected for a functional IHC (fig. S1).

The environment of these transdifferentiated IHCs in the outer compartment, however, was not that of normal IHCs, but composed of the specialized supporting cells characteristic of the outer compartment. In the inner compartment, IHCs are surrounded by three specialized types of supporting cells: IBCs, IPhCs, and IPCs. By contrast, in the outer compartment, the cells providing support to the OHCs are the OPCs and DCs (Fig. 2A). Immunostaining for the Glutamate-Aspartate Transporter GLAST in *Insm1* conditional knockouts (cKOs), which in controls labels IBCs and IPhCs, labeled these types of support cells around the IHCs of the inner compartment, but not around the transdifferentiated IHCs in the outer compartment (Fig. 2B). Immunostaining for PROX1, which labels five rows of support cell nuclei (those of the DCs, OPCs, and IPCs) in controls, labeled the same five rows of supporting cells in *Insm1* cKOs (Fig. 2D). Of those, only the most medial row (corresponding to the IPCs) expressed the IPC marker p75 (Fig. 2C). Hence, the support cells in the outer compartment of *Insm1* cKOs were not IBCs, IPhCs, or IPCs, but OPCs and DCs. The oc-IHCs, given their larger and different shape from OHCs, distort the regular alignment of the outer compartment. However, immunolabeling for α-tubulin, which fills the cytoplasm of pillar cells and DCs, reveals that the oc-IHCs remain within the support cell boundaries of the outer compartment, separated from the tunnel of Corti and the inner compartment (Fig. 2E and fig. S2). We conclude that in *Insm1* cKOs, the oc-IHCs do not induce formation of inner supporting cells (IBCs, IPhCs, and IPCs) around them but are instead surrounded by the supporting cells that normally reside with the OHCs in the outer compartment, namely, the OPCs and DCs. Thus, we have an appropriate model in which to test whether the type of hair cell (IHC versus OHC), or the environment within which it resides (inner versus outer compartment), determines afferent and efferent innervation.

Type I SGNs innervate IHCs situated in the outer compartment

We first asked whether these oc-IHCs receive innervation appropriate to their IHC type (i.e., from type I afferents) or whether this would perhaps be prevented on the basis of their location in the outer compartment, in positions normally occupied by OHCs. We immunostained cochlear whole mounts after hearing onset (P21 to P25) for detection of Calb2, which labels most type I fibers (although in a graded fashion, with higher expression in fibers innervating the pillar side of an IHC) (*42*–*44*). In control animals (either $Atoh1^{Cre/+}$; $Insm1^{F/+}$ or $Insm1^{F/F}$), and consistent with previous findings, Calb2 labeled both IHCs and type I SGN projections that innervate the IHCs (Fig. 3, A to C). No Calb2-positive fibers were observed in the outer compartment at these mature stages. In the absence of INSM1, Calb2-positive type I afferent fibers entered into the organ of Corti as in control (Fig. 3A). However, in contrast to the control, in the cKOs, fibers crossed into the outer compartment and innervated oc-IHCs (Fig. 3, A′ and B, brackets and arrows). Analysis of neonatal organ of Corti revealed that innervation of oc-IHCs was already established by birth (fig. S3).

Not all oc-IHCs were innervated by Calb2-positive, type I afferent fibers. Quantification of oc-IHCs that received Calb2-positive fibers revealed a trend toward cells in the rows closest to the row of IHCs (medial row, no. 1) versus those further away (lateral rows, nos. 2 and 3), being more likely to be innervated by a type I afferent fiber (Fig. 3C). Since this trend only weakly correlated with distance (with an R^2 of 0.4, as measured from the IHC to the oc-IHC; fig. S3B), we postulated that clustered oc-IHCs, which are more common in medial row 1, might emit a greater concentration of neurotrophic or chemoattractant signal to projecting type I afferent fibers. However, the number of fibers received by clustered versus isolated oc-IHCs was not significantly different (fig. S3, C and D). Because OHCs are known to repel type I afferent fibers, an alternative possibility is that, for any given radial position along the organ of Corti, OHCs in row 1 or 2 may prevent type I afferents from reaching oc-IHCs in row 2 or 3. By surface rendering, we examined multiple lateral (third row) oc-IHCs and for each one determined whether it was innervated by Calb2-positive type I afferents and whether an OHC was present in row 1 or 2 (Fig. 3, D and E, with additional examples in fig. S3E). We found that Calb2-positive type I afferents innervated nearly all oc-IHCs for which no OHC stood in the innervation path. In contrast, those afferents that did not innervate the oc-IHCs (with only one exception) faced an interposing OHC (Fig. 3, D and E). These results support the idea that interposing OHCs block type I afferent innervation, which is consistent with the known repulsive cues that are emitted by OHCs, such as ephrin-A5 (*29*) and Semaphorin 3F (*23*).

Together, these findings indicate that type I SGNs are capable of crossing into the outer compartment to innervate oc-IHCs in the absence of an interposing OHC, suggesting that hair cell type, rather than location in the inner versus outer compartment, determines whether type I afferents innervate a cochlear hair cell. IHCs attract type I afferent innervation regardless of location, whereas OHCs repel it.

Ribbon synapses form between oc-IHCs and contacting type I afferents

Concomitant with the arrival of SGN fibers to the IHCs during normal development is the apposition of synaptic ribbons (*45*), electron dense structures that are often surrounded by multiple synaptic vesicles. During the early stages of development, IHCs and OHCs have many ribbon synapses, presumably reflecting the large number of transient afferent fiber connections (*46*). IHCs maintain most of their ribbon bodies, while almost all the ribbons observed in immature OHCs are lost by hearing onset (~P12). Thus, by weaning, IHCs contain 15 to 20 ribbons apposed to AMPA-type glutamate receptors [GluR2/3; (*47*)]. In contrast, OHCs contain one to two larger ribbons that do not localize next to a postsynaptic GluR2/3 afferent terminal (although some of them are apposed to type II collateral terminals) (*48*). As we have shown that oc-IHCs are able to receive type I afferent innervation, we speculated that, unlike their OHC counterparts, they would display an increased number of ribbons and that these

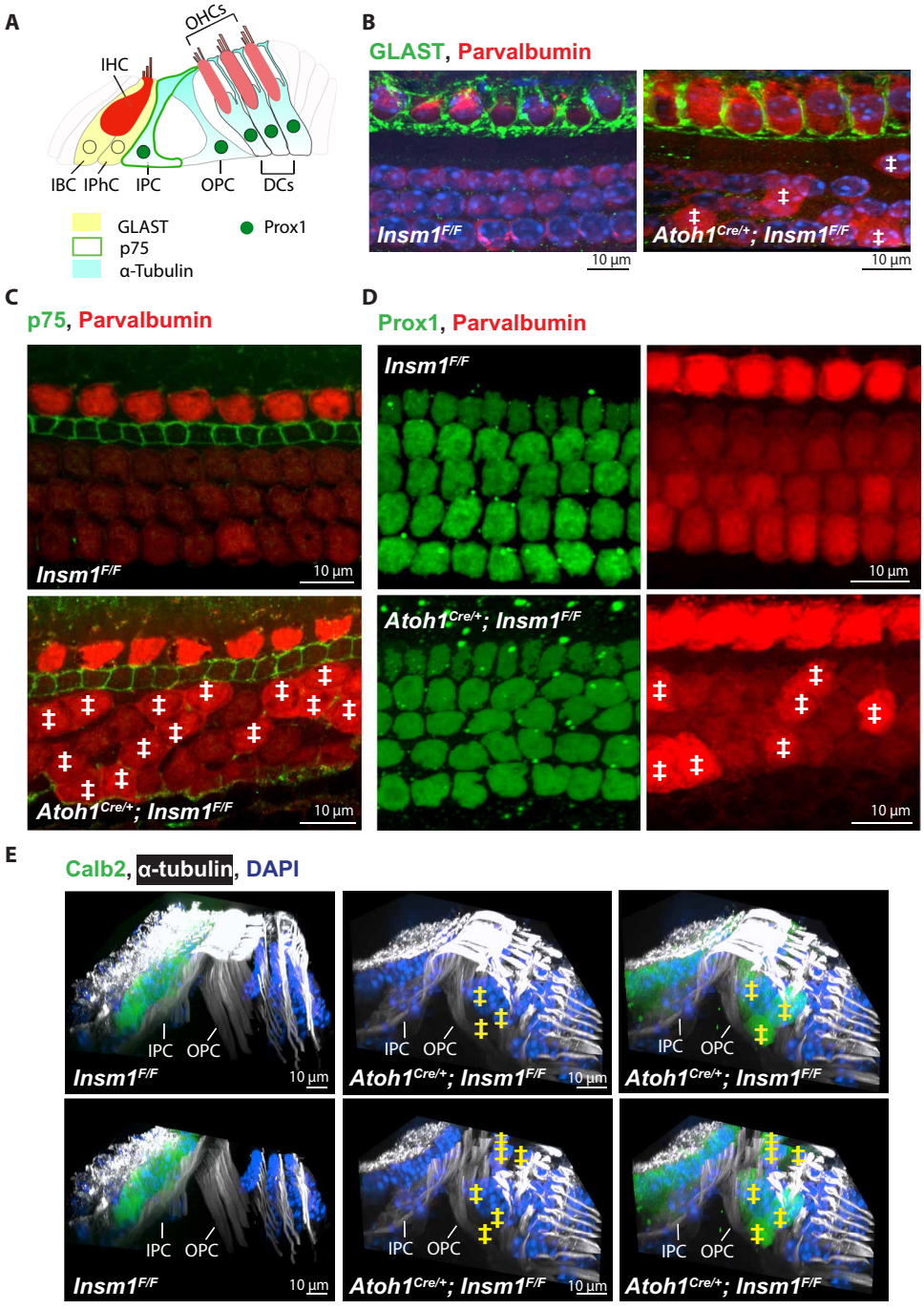

Fig. 2. oc-IHCs are surrounded by outer-compartment, and not inner-compartment, supporting cells. (**A**) Supporting cells in the organ of Corti are identified by their expression of distinct markers, including GLAST (IBCs and IPhCs), p75 (IPCs), Prox1 (in the nuclei of IPCs, OPCs, and DCs), and α-tubulin (IPCs, OPCs, and DCs). (**B** to **D**) Top view of middle turns from P0 control and *Insm1* cKO cochlea, with GLAST labeling IBCs and IPhCs in (B), p75 labeling IPCs in (C), and Prox1 labeling the nuclei of IPCs, OPCs, and the three rows of DCs in (D). Parvalbumin labels IHCs, oc-IHCs, and OHCs (with brighter expression in IHCs and oc-IHCs, where ‡ denotes oc-IHC). (**E**) Side views of middle turns from control and cKO adult cochlea, with α-tubulin labeling the IPCs, OPCs, and DCs. IPCs and OPCs separate cells in the inner compartment from those in the outer compartment in both control and mutant cochlea. The lower panel has the top sections removed to better visualize the IPC and OPC columnar processes. Calb2 labels IHCs and oc-IHCs (denoted with ‡). DAPI, 4′,6-diamidino-2-phenylindole.

would have established synapses with type I afferent terminals expressing GluR2/3 receptors.

We immunostained cochlear whole mounts for pre- and postsynaptic markers at weaning (P21 to 25). In control animals, IHCs have multiple CtBP2 (C-terminal binding protein 2)–positive puncta (red, representing presynaptic ribbons) apposed to GluR2/3-positive puncta (green, representing postsynaptic receptor plaques) (Fig. 4A). In control OHCs, there are significantly less CtBP2-positive puncta,

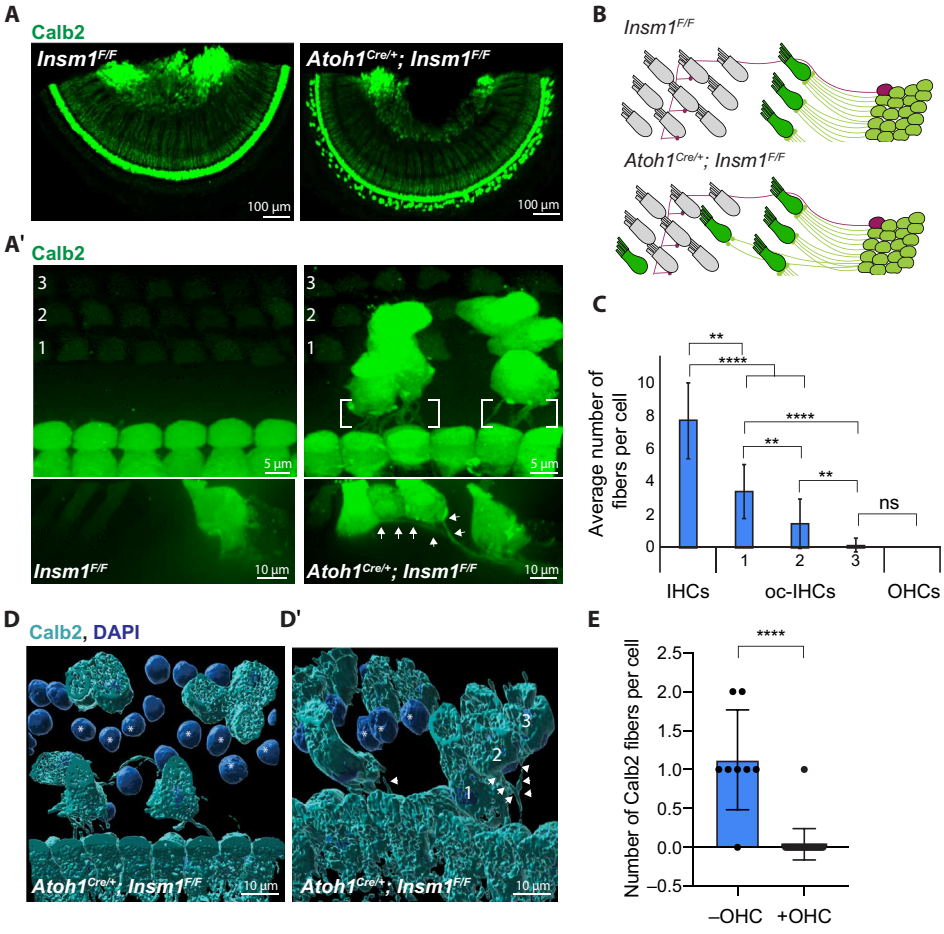

Fig. 3. Type I afferents innervate IHCs situated in the outer compartment (oc-IHCs) as long as they do not encounter an interposed OHC. (**A** and **A′**) Top views of Calb2-labeled IHCs, oc-IHCs, and type I SGNs from a middle turn of control or *Insm1* cKO adult cochlea. Calb2-labeled fibers are not in the outer compartment of controls (A and A′). In cKOs, Calb2-labeled fibers extend toward and innervate the oc-IHCs (brackets or arrows). (**B**) Type I SGNs (green) form a single connection with IHCs, while type IIs (purple) cross into the outer compartment and send multiple collateral projections that each connect with an OHC. In mutants, type I afferents cross into the outer compartment to form connections with oc-IHCs. (**C**) Calb2-labeled fibers are more likely to innervate oc-IHCs closest to the IHC row, with fewer cells receiving type I innervation in the row furthest from the IHCs (****$P < 0.0001$, **$P < 0.005$, and ns, $P > 0.99$; Kruskal-Wallis test with Dunn's multiple comparisons; $n \geq 30$ cells from ≥4 cochleae, error bars = SD). (**D** and **D′**) Three-dimensional (3D) reconstructions of Calb2-labeled fibers and IHCs from cKOs (middle turns). oc-IHCs in rows 2 and 3, furthest from the IHCs, do not receive type I afferent innervation when OHCs (asterisks) are in the way. In contrast, in the absence of interposed OHCs, oc-IHCs in rows 2 and 3 receive type I afferent innervation (arrowheads, D′). (**E**) oc-IHCs in row 3 are often (8 of 9) innervated in the absence, but rarely (1 of 25) in the presence, of an interposed OHC ($P < 0.0001$, Mann-Whitney test, error bars = SD).

which are never apposed to GluR2/3. In mutants, in addition to colocalized CtBP2 and GluR2/3 in the IHCs, we also observed a clear apposition in the oc-IHCs (Fig. 4, A and A′). Quantification of control and mutant organs of Corti revealed that oc-IHCs have more ribbons than OHCs, but a reduced number compared to the normal IHCs (Fig. 4B). In addition, oc-IHCs in the lateral (second and third) rows have fewer ribbons than oc-IHCs in the medial (first) row (2.8 and 2.4 versus 5.3 ribbons per cell, respectively), as well as a reduction in the number of CtBP2-positive puncta that colocalize with GluR2/3 (around 56% in row 1 versus 27% in row 3; Fig. 4C). We next asked whether the lower number of ribbons in lateral-row versus medial-row oc-IHCs was a direct consequence of their reduced type I afferent innervation (as shown in Fig. 3C). We found significantly more ribbons in lateral-row oc-IHCs that receive type I afferent fibers than in those with no detectable type I afferent connection (Fig. 4, D and E). Furthermore, this latter group of oc-IHCs was statistically indistinguishable from that of the OHCs (with around 6 ribbons per cell in innervated oc-IHCs versus 1.5 in oc-IHCs that did not receive innervation and 1.4 ribbons per cell in OHCs). We conclude that oc-IHCs form synapses with type I afferents if contacted by them.

In nearly all features examined, oc-IHCs are indistinguishable from IHCs of the inner compartment (table S1 and fig. S1). Hence, we wondered why innervated oc-IHCs, while establishing ribbon synapses with type I afferents, did not have nearly as many synapses as the normal IHCs of the inner compartment. It is well established that each type I afferent contacts only one IHC and forms 1 to 2 ribbon synapses, so that each IHC has, depending on its apical-basal position, between 10 and 20 ribbons (*9*, *47*, *49*–*51*). Given that there is a fixed number of type I afferent SGNs, we would expect that if some of them contact oc-IHCs, then fewer would contact the normal IHCs at the same radial positions. Accordingly, quantification of the number of ribbon synapses reveals that IHCs of *Insm1* cKOs have fewer

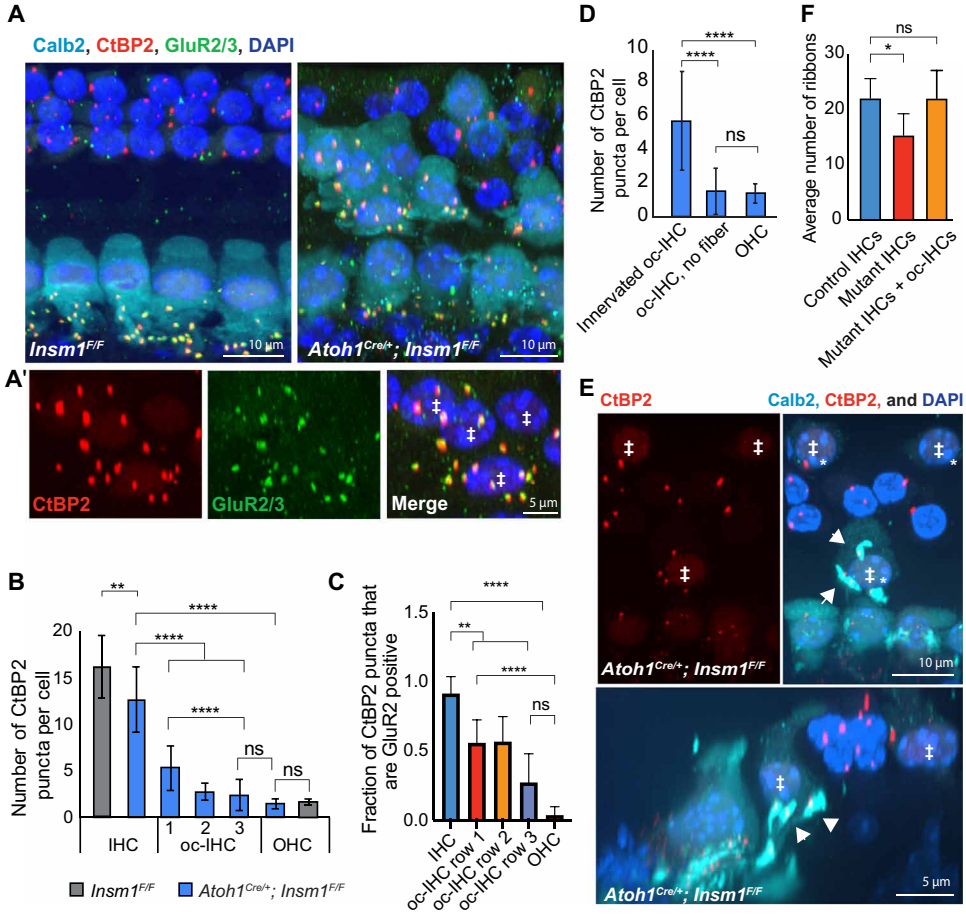

Fig. 4. Ribbon synapses form between oc-IHCs and innervating type I afferents. (**A**) Top view of control and *Insm1* adult cKOs (middle turns) with Calb2-labeled IHCs and oc-IHCs (‡ in **A'**) and CtBP2- and GluR2/3-juxtaposed puncta distinguishing ribbon synapses. oc-IHCs have juxtaposed CtBP2 and GluR2/3 puncta like IHCs (A, right, magnified in A'), while OHCs have one to two ribbons but these are not apposed to GluR2/3. (**B**) oc-IHCs in row 1 have more ribbons than oc-IHCs in rows 2 and 3 (****$P < 0.0001$, **$P = 0.002$, and ns, $P > 0.6$; one-way analysis of variance (ANOVA) with Tukey's multiple comparisons test; $n \geq 110$ cells per condition; from >6 animals; error bars = SD). (**C**) oc-IHCs have fewer juxtaposed CtBP2-positive and GluR2/3-positive puncta compared to IHCs, but significantly more than OHCs ($n \geq 18$ cells per condition; from four cochlea, ****$P < 0.0001$, **$P < 0.005$, and ns, $P > 0.1$; error bars = SD). (**D**) oc-IHCs that receive type I innervation have more CtBP2-labeled ribbons than oc-IHCs that are not innervated (****$P < 0.0001$ and ns, $P > 0.99$; Kruskal-Wallis test with Dunn's multiple comparison test; $n > 85$ cells; from >6 cochlea; error bars = SD). (**E**) Top and side views of a basal turn from an *Insm1* cKO with CtBP2-labeled ribbons and Calb2-labeled IHCs, oc-IHCs (‡) and type I SGN fibers/terminals (arrowheads). The number of presynaptic ribbons (red) in each oc-IHC correlates with the number of postsynaptic terminals (cyan). The two oc-IHCs in the row furthest from the IHCs do not receive a type I SGN terminal and have an OHC-like number of ribbons. (**F**) The number of ribbons in IHCs was lower in mutants than in controls, but comparable when adjacent oc-IHCs from the same radial segment were taken into account (*$P = 0.0298$ and ns, $P > 0.99$; Kruskal-Wallis test with Dunn's multiple comparison test; $n = 5$ segments per condition; from five cochlea; error bars = SD).

than those of controls, but that the total number of ribbon synapses remains the same between control IHCs and mutant IHCs plus innervated oc-IHCs (Fig. 4F). It appears that oc-IHCs compete with inner compartment IHCs for innervation and ribbon synapse formation by the limited number of type I afferents.

Efferents approaching IHCs in the outer compartment terminate axodendritically on type I afferents

We next sought to analyze the olivocochlear efferent innervation of oc-IHCs, making use of an antibody against vesicular acetylcholine transporter (vAChT, present in all cholinergic neurons) that labels most efferent terminals in the cochlea. In control animals, vAChT-positive efferent terminals appear as multiple dispersed small puncta (each averaging around 3 μm^3; fig. S4), indicative of their axodendritic termination on type I afferent fibers under the IHCs. In the OHCs, vAChT puncta are large (with an average volume of 21 μm^3; fig. S4) and localize immediately adjacent to the basal end of the OHCs (Fig. 5A), indicative of the axosomatic termination of efferents directly on the hair cells. In mutants, IHCs and OHCs have efferent terminal patterns (both distribution and size) comparable to that of control animals. However, oc-IHCs were rarely adjacent to the large vAChT signal indicative of axosomatic efferent termination. Instead, under most oc-IHCs, we observed the vAChT pattern that is indicative of axodendritic efferent terminals: small dispersed puncta in close contact with the type I afferent fibers projecting to the oc-IHCs (Fig. 5A, bottom, between brackets). These puncta are, on average, around 3 μm^3 (fig. S4), indistinguishable from the volume of puncta under control IHCs.

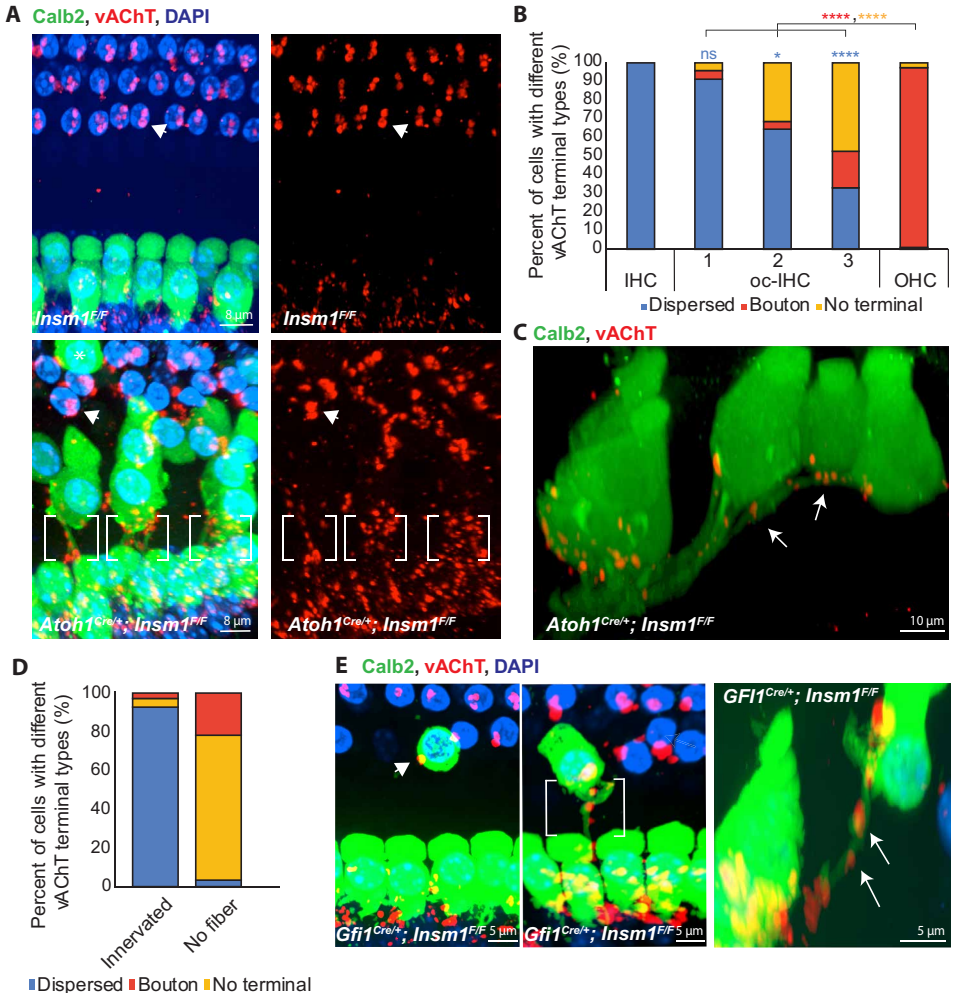

Fig. 5. Efferents terminate axodendritically on type I afferents innervating oc-IHCs, rather than axosomatically on the hair cells. (**A**) Top views of adult control (top) and *Insm1* cKOs (bottom) with Calb2-labeled IHCs, oc-IHCs and type I SGNs, and vAChT-labeled efferent terminals. Most oc-IHCs in row 1 have an IHC-like efferent termination pattern with small, dispersed vAChT-positive puncta decorating Calb2-labeled type I fibers projecting into the outer compartment (brackets) versus the larger axosomatic boutons associated with OHCs (arrowheads). oc-IHCs in row 3 (asterisk) often do not have OHC-like efferent termination. (**B**) oc-IHCs in row 1 have small, dispersed (axodendritic-like) vAChT terminals. Row 3 oc-IHCs often have no vAChT-positive efferent terminal or, less often, receive a larger axosomatic-like vAChT-positive terminal (ns, $P > 0.9$, $^{*}P = 0.0056$, and $^{****}P < 0.0001$; blue *P* values denote comparisons of IHCs versus rows 1 to 3 for dispersed puncta, while OHC versus row 1 to 3 comparisons are indicated in red (boutons) or orange (no termination); one-way ANOVA with Tukey's multiple comparisons test; $n \geq 67$; from six adult animals). (**C**) Side view of hair cells from the middle turn of an adult *Insm1* cKO with Calb2-labeled IHCs, oc-IHCs, and type I afferents. vAChT-labeled efferent terminals decorate the type I afferent fibers reaching the oc-IHCs in all three rows (arrows). (**D**) Type I afferents innervating oc-IHCs receive dispersed axodendritic innervation. oc-IHCs that do not receive a type I afferent fiber are either not innervated by efferents (75%) or have clustered efferent endings characteristic of axosomatic terminals (21%; $P < 0.0001$, Mann-Whitney test; $n \geq 28$; from six adult animals). (**E**) Top and side views of middle turns from $Gfi1^{Cre/+}$;$Insm1^{F/F}$ adult cochlea. oc-IHCs without type I afferent innervation receive axosomatic efferent termination (arrowhead), while oc-IHCs that receive a type I fiber have axodendritic efferent termination (brackets and arrows).

Quantification revealed that oc-IHCs in medial row 1 were more likely to receive the axodendritic termination pattern than oc-IHCs in lateral rows 2 and 3 (Fig. 5B). This efferent distribution mimics that of type I afferents on oc-IHCs. Consistently, the few oc-IHCs in lateral row 3 observed to have axodendritic efferent termination corresponded to those that also received type I afferent innervation (Fig. 5C, with an additional example shown in fig. S4B). To test for a correlation, we assessed efferent termination type in cells that either received Calb2-positive (type I) afferent fibers or not. Almost all the cells innervated by type I afferents were associated with small and dispersed vAChT puncta (77 of 83 cells; 93%), consistent with the characteristic axodendritic efferent termination (Fig. 5D). In contrast, among the oc-IHCs that were not innervated by Calb2-positive type I afferents, only 1 of 28 cells was associated with multiple, small vAChT puncta under the hair cells (Fig. 5D). This one exception could either reflect an oc-IHC innervated by a Calb2-negative type I afferent or a stray efferent fiber passing under a noninnervated cell. Curiously, most of the oc-IHCs that were not innervated by $Calb2^{+}$ type I afferents received either no efferent termination (21 of 28 cells; 75%) or the axosomatic termination characteristic of OHCs (6 of 28 cells; 21%) (Fig. 5D).

As *Atoh1* is expressed in the hindbrain (*17*), a concern was that the effects that we observe may be due to a direct effect on the efferents themselves. However, since efferent connection to control

IHCs (in the inner compartment by LOCs) and OHCs (by MOCs) is normal (Fig. 5A), this possibility seems unlikely. Nonetheless, for definitive proof, we targeted *Insm1(Flox)* ablation with the knock-in line *Gfi1-Cre*, which is not expressed in the brainstem (*52*). In *Gfi1*$^{Cre/+}$*; Insm1*$^{F/F}$ cKOs, oc-IHCs also had axodendritic efferent termination when contacted by a type I afferent fiber (Fig. 5E, top-view brackets and side-view arrows), and either axosomatic efferent termination (Fig. 5E, top-view arrowhead) or no efferent termination (not shown) in the absence of a type I afferent fiber. We conclude that when oc-IHCs are innervated by type I afferents, the incoming efferents terminate axodendritically on the nerve fibers instead of axosomatically on the hair cells. What remains to be elucidated is what determines, in the absence of type I afferent innervation, whether an oc-IHC receives axosomatic efferent innervation or no efferent innervation at all.

Axodendritically terminating efferents in the outer compartments are MOCs, not LOCs

In normal ears, the only efferents terminating axodendritically are LOC efferents at the inner compartment, whereas the only efferents innervating the outer compartment are MOC efferents ending axosomatically. We reasoned that the contacts under the oc-IHCs could either be LOC fibers crossing into the outer compartment to innervate afferents under the oc-IHCs, or MOC fibers that terminate axodendritically on any type I afferent fibers that they encounter in the outer compartment. We first assessed this using a known marker of LOC efferents, tyrosine hydroxylase (TH). TH-positive fibers represent a subgroup of LOC efferents (around 10 to 20% of all efferent fibers projecting to the mature inner compartment) that, under normal physiological conditions, do not express vAChT. While vAChT labeling is continuous throughout the cochlea, TH innervation is spotty and discontinuous (*53*). For example, regions in the cochlea that have TH-labeled fibers reaching (and spiraling underneath) the row of IHCs (the inner spiral bundle, or ISB), are often flanked by stretches in which TH-labeled fibers approach but do not reach the ISB. To account for this variability, we restricted our analysis to regions of the cochlea in which the TH-labeled fibers reached the ISB (Fig. 6, A and B). In control mice, we did not observe any TH-positive fibers crossing into the outer compartment (Fig. 6A). Likewise, in mutants, the vast majority of fibers did not project toward the oc-IHCs (104 of 107 oc-IHCs counted from six independent cochleae). Only on one occasion (in the third turn of a single cochlea) did we observe a TH-positive fiber crossing into the outer compartment and passing underneath three oc-IHCs in row 1 (Fig. 6B).

The above reveals that the efferent fibers terminating axodendritically on type I afferents under the oc-IHCs are not (in >97% of cells examined) LOC efferents of the TH-positive subtype. We next wondered whether they are another type of LOC efferent or, alternatively, MOC efferents (which are the only efferents that normally innervate the outer compartment). To discern between these two possibilities, we performed double immunohistochemistry with an antibody to Na^+- K^+-adenosine triphosphatase α3 (Na^+/K^+-ATPase α3) [which labels MOC fibers and type I afferents, but not LOC fibers; (*28*, *54*)], in conjunction with an antibody to calcitonin-gene-related peptide (CGRP) [which labels both LOCs and MOCs (*55*)]. In control animals, we observed robust colabeling of Na^+/K^+-ATPase α3 and CGRP in tunnel crossing efferent fibers (all of which are known to be MOCs) and terminals in the outer compartment (Fig. 6C, top). By contrast, in the inner compartment of control animals, traveling radially toward the IHCs and spiraling under them, presumed LOC fibers were labeled with CGRP and not Na^+/K^+-ATPase α3 (fig. S5A, arrows and #). Conversely, many radial Na^+/K^+-ATPase α3–labeled fibers were CGRP negative, as expected for type I afferents (fig. S5A, *). In the cochleae of *Insm1* cKOs, all tunnel crossing efferent (CGRP-positive) fibers and terminals were immunolabeled with the MOC marker Na^+/K^+-ATPase α3 (type I fibers projecting to the oc-IHCs were also identifiable as Na^+/K^+-ATPase α3-positive and CGRP-negative, fig. S5B). Importantly, all CGRP-positive fibers projecting toward oc-IHCs were colabeled with Na^+/K^+-ATPase α3 (Fig. 6C, bottom). Together, our data suggest that LOC fibers do not cross into the outer compartment in the presence of oc-IHCs. Rather, MOC fibers innervating the outer compartment terminate axodendritically if they encounter a type I afferent innervating an oc-IHC.

Type II afferents can innervate IHCs in the outer compartment

Our data so far reveal that type I afferents innervate IHCs in the outer compartment as long as there is not an OHC in the way. To visualize type II afferents, we performed immunohistochemistry to detect peripherin, an intermediate filament that marks the primary fibers of type II afferents robustly up to around P7 (after which expression begins to diminish in the type II processes, although it is retained in the soma). In *Insm1* cKOs, as in controls, type II afferent fibers cross into the outer compartment, turn toward the base, and extend their processes underneath the OHCs but also under the intercalating oc-IHCs (fig. S6, A and B; white arrows denote turning toward the base). However, compared with the three parallel bundles of spiraling type II afferents in controls, the mutants displayed a reduction of bundling and a disorganization of the spiraling type II fibers. These results are to be expected, given that the presence of bulky oc-IHCs disrupts the alignment of outer compartment rows of HCs and surrounding supporting cells (Fig. 2 and fig. S2). However, the presence of oc-IHCs in the position of OHCs did not act as a barricade for type II afferents, which bypassed the oc-IHCs to project radially and turn spirally as in the controls.

At maturity in wild-type mice, type IIs are the sole afferents projecting into the outer compartment to innervate OHCs. We thus wondered whether type II fibers would innervate oc-IHCs. Since the antibody to peripherin does not label the collateral projections that extend from type II primary fibers to innervate the OHCs, we labeled immunohistochemically for parvalbumin. Parvalbumin marks both type I and II processes (including type II collaterals), but these are clearly distinguished on the basis of anatomical features: Type I afferent fibers approach hair cells radially, whereas type II afferent fibers run spirally under the hair cells and send collateral projections upward to innervate the OHCs (*43*) (Fig. 7A, top). By immunolabeling for Calb2 (type I afferents) and parvalbumin (all afferents), we found that none of the oc-IHCs innervated by type I afferents received type II afferent innervation (n = 44 oc-IHCs). It has been hypothesized that type II afferents, which bypass IHCs on their way toward the outer compartment, do not innervate them because of competition from type I afferents (*29*). Hence, we wondered whether the 28% (63 of 228) of oc-IHCs that are not innervated by type I afferents could receive type II innervation. In *Insm1* mutants, spiraling type II afferents sent collaterals to contact OHCs. Notably, collaterals also extended to and contacted some oc-IHCs (Fig. 7, A′ and C, top). In young animals (P10, the earliest stage at which we have been able to visualize type II collaterals with anti-parvalbumin), all the examined oc-IHCs that were not innervated by type I afferents

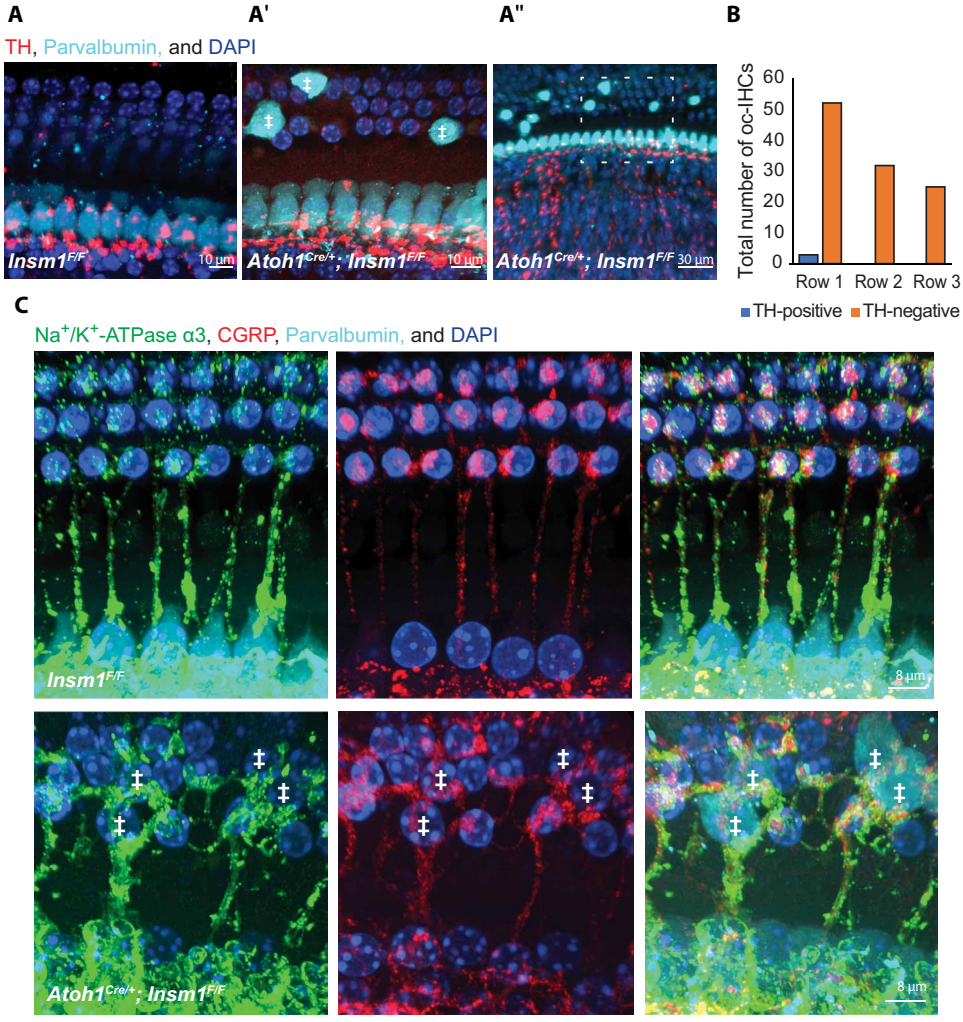

Fig. 6. Axodendritic efferents terminating on type I afferents innervating oc-IHCs are MOCs, not LOCs. (**A**) Top view of middle turns from control (A) and *Insm1* adult cKO cochlea (**A′** and **A″**) with Parvalbumin labeling IHCs and oc-IHCs (‡), and TH labeling a subgroup of LOC fibers. TH-positive LOC fibers do not cross into the outer compartment to innervate oc-IHCs. A′ is a magnified version of A″ (shown by dashed box). (**B**) Quantification of oc-IHCs from adult *Insm1* cKOs that are in apparent contact with TH-labeled fibers. All counting was performed in regions of a given cochlea where TH-positive fibers reached the ISB (running under the IHC row). (**C**) Top view of adult control (top) and cKO (bottom) cochleae from middle turns with Na^+/K^+-ATPase α3 labeling MOC efferents and type I afferents (*28*, *54*), and CGRP labeling both LOC and MOC efferents. Parvalbumin labels IHCs and oc-IHCs (‡). In both control and mutant animals, all efferent (CGRP-positive) fibers that cross into the outer compartment are colabeled for Na^+/K^+-ATPase α3, suggesting that they are MOC fibers.

were contacted by a type II afferent fiber collateral (Fig. 7, A′ and B). By P15, we observed a reduction in the number of oc-IHCs contacted by type II afferents to around 63%, while in mature cochleae, only 35% of the third-row oc-IHCs received type II afferent contacts (Fig. 7B). The remaining 65% were not contacted by collateral projections. These oc-IHCs were not innervated by afferents of any type (Fig. 7, A″ and C, bottom), although some were observed to have remnants or fragments of collaterals close by (Fig. 7A″, bottom, white arrows). This suggests that when type II fibers pass under IHCs in the outer compartment, they send collaterals and establish contact with oc-IHCs. However some of these contacts are lost as maturation proceeds. We conclude that type II afferents can innervate IHCs (even if in some cases this is transient) when these are in the outer compartment and are not innervated by type I afferents.

The type of afferent neuron determines whether efferents innervate and how they terminate

Thus far, we have found that oc-IHCs that are innervated by type I afferents are subject to axodendritic efferent innervation. Of the remaining oc-IHCs, some were innervated axosomatically by efferents, whereas others had no efferent innervation. We wondered whether either of these were the same oc-IHCs that received type II afferent collateral innervation (i.e., whether there was a correlation between type II afferent and axosomatic efferent innervation). We focused our analysis on outer-row oc-IHCs that did not receive type I afferent innervation (since they are more prevalent in this outer row). Using Imaris, we rendered surfaces of parvalbumin-labeled type II fibers from control or mutant organs of Corti. In mature cochleae, we observe clear examples of oc-IHCs that either do or do not receive a parvalbumin-labeled collateral (Fig. 7C). The oc-IHCs

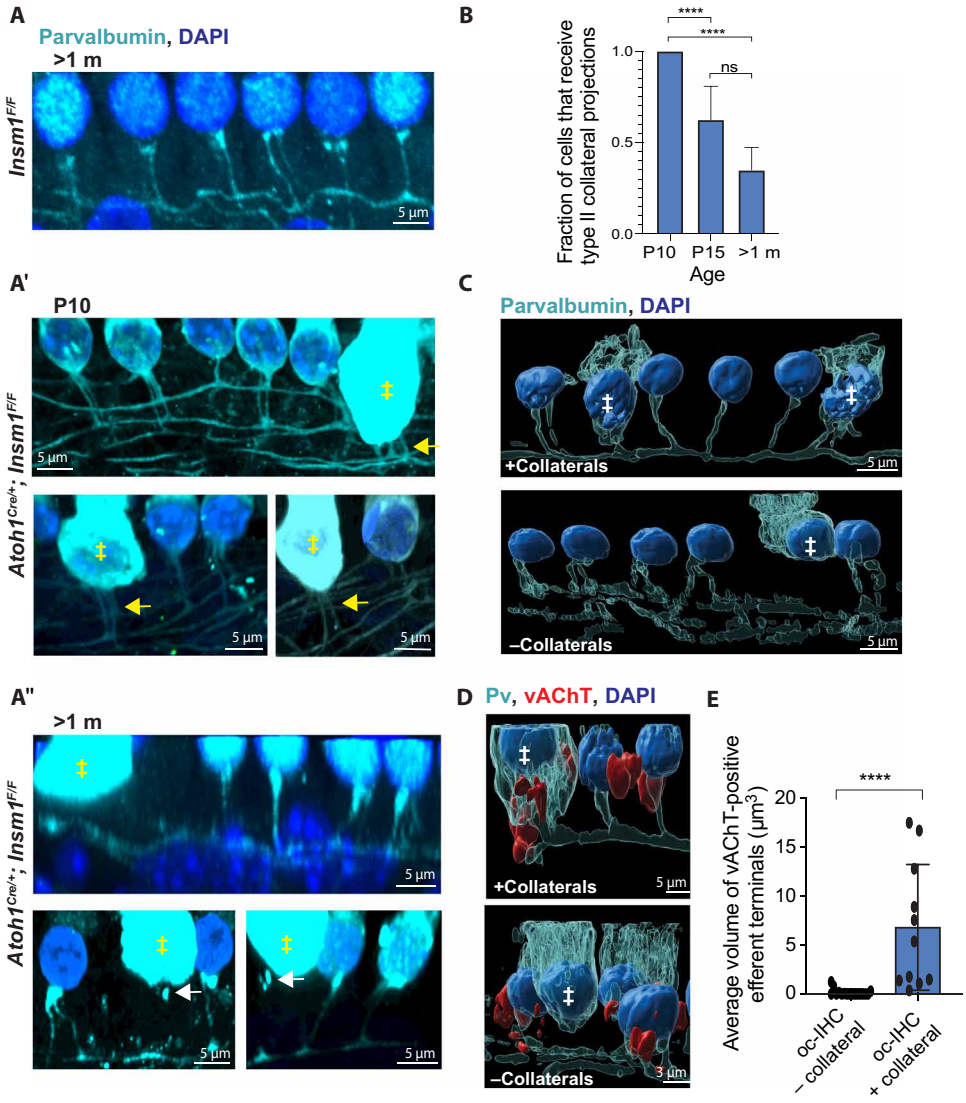

Fig. 7. Co-occurrence of type II afferent and axosomatic efferent innervation in oc-IHCs. (**A** and **B**) Side view of control (A) and *Insm1* cKO third-row outer-compartment HCs at age P10 (**A′**, from basal turns) or P35 (A and **A″**, from middle turns). Parvalbumin labels HCs (oc-IHCs stronger than OHCs) and type II collaterals. At P10, OHCs and oc-IHCs (‡) receive at least one collateral projection (A′, arrows). At P35, OHCs receive type II afferent innervation, but the oc-IHC shown (‡) in the top panel does not (A″). In the lower panels, the oc-IHCs (‡) have only fragments of former collaterals (arrows). (**B**) oc-IHCs (not contacted by a type I afferent) are innervated by type II collaterals early in development (P10), but by maturity (P30 to P42), many oc-IHCs lack them (****$P < 0.0001$, binomial test; $n \geq 15$; from three to five animals; error bars = SD). (**C** and **D**) 3D reconstructions of parvalbumin-positive type II fibers and collaterals showing examples of mature (P30 to P42) oc-IHCs (‡) that maintain collaterals (+collaterals) or have lost them (–collaterals). (D) Colabeling for vAChT reveals an oc-IHC innervated by both a type II afferent collateral and an efferent (terminating axosomatically; left), as well as an oc-IHC receiving neither type II afferent nor efferent innervation (right). (**E**) Cells receiving type II collateral projections receive large vAChT efferent terminals, whereas cells without type II collaterals lack efferent terminals [****$P < 0.0001$, Mann-Whitney test; $n \geq 11$ from four to five animals (P18 to P35); error bars = SD].

are distinguished by their cytoplasmic parvalbumin staining, which is much stronger than in neighboring OHCs. Parallel rendering of surfaces for the costained efferent marker vAChT revealed that oc-IHCs innervated by a type II afferent collateral were also contacted by a large, vAChT-labeled efferent terminal. In contrast, in oc-IHCs lacking a type II afferent contact, vAChT-labeled terminals were either missing or of negligible size (<3 µm^3; Fig. 7, D and E). Thus, innervation of oc-IHCs by type II afferent correlates with axosomatic innervation by efferents.

We have shown that oc-IHCs innervated by type I afferents are subject to axodendritic efferent innervation, oc-IHCs innervated by type II afferents receive axosomatic efferent innervation, and oc-IHCs not innervated by afferents also lack efferent innervation. Given that afferent innervation of hair cells predates the arrival of efferent fibers (*20*, *23*–*25*, *34*, *56*, *57*), it seems that afferent innervation determines whether and how efferents will innervate. For additional proof, we examined the afferent innervation pattern in organotypic cultures of the cochlea, in which the efferents are absent. We explanted cochleae at P2, before the arrival of efferents [P3 to the inner and P6 to the outer compartments; (*24*)], cultured 6 days in vitro (to the equivalent of P6 to P8), and then examined the afferent innervation of hair cells. Using Calb2 to label type I afferent fibers,

we observed projections to the IHCs in control explants, with no crossing into the outer compartment, as expected. In contrast, in mutant explants, we observed crossing events, with type I afferent fibers projecting to the oc-IHCs (fig. S7). Hence, type I afferent innervation of the oc-IHCs can occur in the absence of efferent innervation in explant culture. Because type II afferent collaterals are not observable in our hands until P10 (the earliest we can label them with anti-parvalbumin), and we cannot culture cochlea this late in development, we are unable to similarly confirm whether type II afferent innervation can occur in the absence of efferents. However, given that animals without efferents formed and maintained type II afferent innervation (*58*) (see Discussion below), it follows that these neurons must also be able to innervate the oc-IHCs in the absence of efferents.

In summary, by examining the innervation of *Insm1* conditional mutants, in which there are IHCs in the place of OHCs, we find that (i) type I afferents will cross into the outer compartment and establish synaptic contacts with IHCs, (ii) intervening OHCs prevent this innervation, (iii) type II afferents can innervate IHCs if they are not innervated by type I afferents, (iv) efferents innervating the outer compartment are MOC efferents, not LOC efferents, but (v) the type of afferent innervating the IHC predicts how the efferent innervation terminates: Type I afferent innervation results in axodendritic efferent ending, type II afferent innervation results in axosomatic ending, and no (or loss of) afferent innervation results in no (or loss of) efferent ending (Fig. 8, A to C).

DISCUSSION

Together, our results suggest a hierarchical logic for the development of the organ of Corti's innervation circuitry (Fig. 8D). First, hair cell type instructs afferent innervation as follows: IHCs attract, and OHCs repel, type I afferents. Type II afferents can innervate both OHCs and IHCs, but the preferred innervation of IHCs by type I afferents supersedes innervation by type II afferents. Second, the type of afferent innervating a given hair cell does not determine what type of efferent will innervate (LOC fibers innervate HCs within the inner compartment and MOC fibers innervate HCs within the outer compartment) but does determine the way it will terminate: Type I afferents induce axodendritic efferent termination on themselves, while type II afferents induce axosomatic efferent endings on the hair cells. Last, afferents seem to be required for efferent innervation, because when they are lost from HCs, the efferent connections also disappear.

Hair cell type determines afferent innervation

In *Insm1* mutants, the supporting cells around the oc-IHCs are those of the outer compartment (OPCs and DCs) and not those that normally surround IHCs in the inner compartment (IBCs, IPhCs, and IPCs). Hence, the finding that type I afferents innervate IHCs even if located in the outer compartment implies that an inherent property of these hair cells, rather than their environment (i.e., the inner compartment), prompts their innervation by type I afferents. IHCs attract type I afferents, or at least they are more permissive to their innervation than other cells in the organ of Corti (OHCs and the various types of supporting cells), regardless of location (i.e., the inner or outer compartment). It remains to be elucidated what the IHC chemoattractant might be. Conversely, our observation that any OHC located between an approaching type I afferent fiber and an oc-IHC prevents the latter from receiving type I afferent innervation is in keeping with the reported chemorepulsion that OHCs effect on these neurons. For example, OHCs produce at least two ligands (ephrin-A5 and Semaphorin 3F) that repel type I afferent neurites (*23*, *29*). Hence, the selective innervation of IHCs by type I afferents likely results from a combination of attractive cues from IHCs and repulsive ones from OHCs.

We find that type II afferents still innervate the outer compartment of *Insm1* mutants, despite the fact that half of the hair cells are IHCs. These fibers turn normally toward the base of the cochlea and even send out collateral projections that innervate the misplaced oc-IHCs. This finding reveals that the compartment in which the hair cells reside, rather than the type of hair cell (outer versus inner), determines the innervation pattern of type II afferents. This is consistent with reports that type II afferent innervation is guided by signals from supporting cells (*33*, *59*–*62*) and contrary to what we have found for type I afferents.

In the absence of Eph/ephrin signaling, type I fibers overshoot into the outer compartment and result in a withdrawal of type II afferent projections from the OHCs (*29*). From this, it has been proposed that type II afferents may be capable of innervating IHCs but that they fail to do so because of competition from type I afferents. Testing this prediction has been awaiting a model lacking IHCs innervated by type I afferents. The *Insm1* cKOs offer such a model, with some IHCs in the outer compartment not innervated by type I afferents. The innervation of these IHCs by type II afferents provides definitive evidence that synapses between them are indeed possible.

The lack of IHCs with dual innervation by both type I and II afferents, and the fact that what prevents type I afferent innervation of oc-IHCs is OHC chemorepulsion, supports the idea that innervation of IHCs by type I afferents impedes innervation by type II afferents. We can rule out inhibition of type II innervation by the local environment or by an inherent chemorepulsion from the oc-IHCs since oc-IHCs did not cause a change in the local environment (outer supporting cells did not change into inner supporting cells) and since type II fibers were able to make contact with some oc-IHCs (those not innervated by type I afferents). Speculatively, we suggest that type I fibers may emit (or induce the IHCs that they innervate to emit) chemorepulsive cues that prevent type II fibers from making connections with IHCs. Alternatively, type 1:IHC connections may be more favorable and/or stable than type II:IHC connections, thus outcompeting them.

Afferent innervation determines efferent termination

The innervation of IHCs in the outer compartment of *Insm1* cKOs by MOC fibers and not LOC fibers reveals that the innervation of the outer versus inner compartment by efferent fibers is not determined by the type of hair cell residing there, but by either the type of efferent (defined on the basis of the location of its soma in LSO or MSO) and/or by the compartment (inner versus outer) of the organ of Corti being innervated. However, a series of results indicate that how the MOC efferents terminate is not an inherent property of this type of neuron and is not dependent on the type of hair cell that they innervate (OHC versus IHC) nor on the compartment where the target hair cell resides (inner versus outer). Instead, whether and how MOCs terminate can be predicted by the type of afferent neuron innervating the hair cell.

First, we find that MOC efferents approaching oc-IHCs that are innervated by type I afferents terminate axodendritically on these afferents instead of axosomatically on the hair cells (as is characteristic

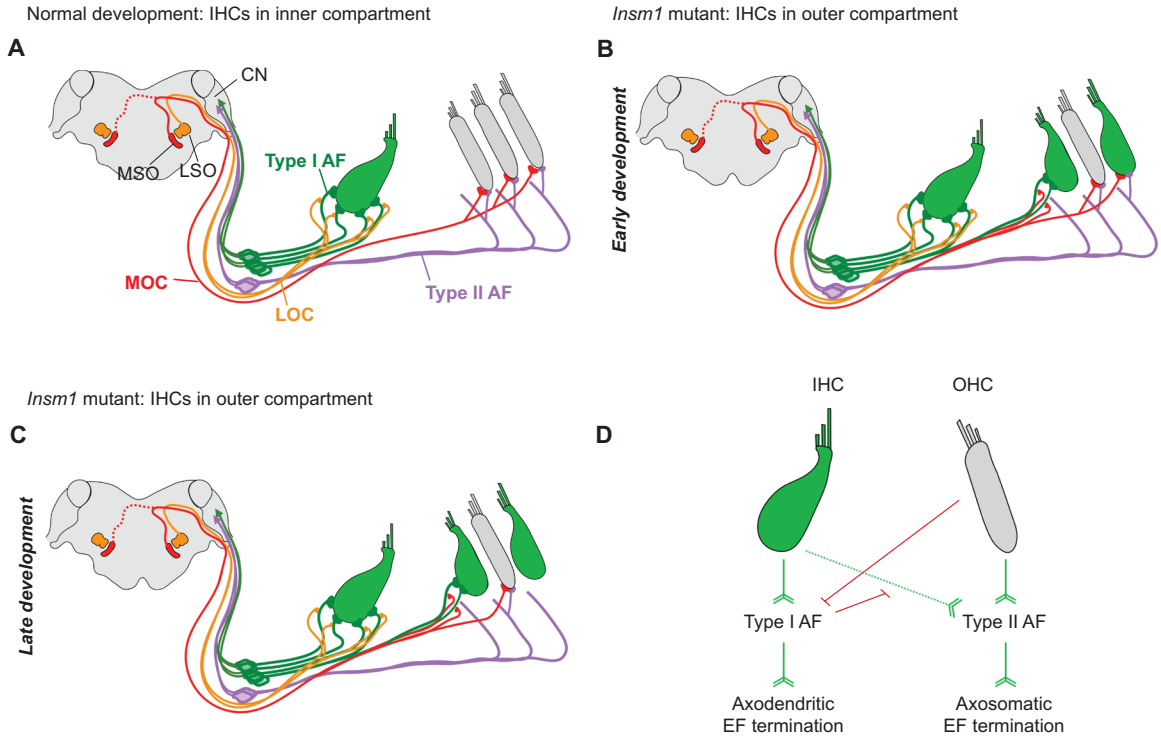

Fig. 8. Schematic illustration and hierarchical model of organ of Corti innervation. (**A**) In mature control cochleae, LOC efferents (orange) make axodendritic connections to type I afferent fibers (green) projecting to IHCs (green). Type II afferents (purple) cross into the outer compartment, turn basally, and send collateral projections to a number of OHCs (gray). MOC efferents (red) make axosomatic connections with OHCs. The MSO, LSO, and cochlear nucleus (CN) are indicated. (**B**) In *Insm1* cKO cochleae, type I afferents (AF) cross into the outer compartment to innervate oc-IHCs when there are no interposed OHCs. MOCs make axodendritic connections with type I afferents projecting to these oc-IHCs. oc-IHCs not innervated by type I afferents instead receive collateral projections from type II afferents. These cells also maintain axosomatic connection with MOC fibers, similar to surrounding OHCs. Over the course of development, many type II connections with oc-IHCs are lost, resulting in oc-IHCs not innervated by type I or II afferents (**C**). These cells also lose efferent connections. Hence, efferent termination depends on the type of afferent fiber connecting the HCs. (**D**) Hierarchical logic for the development of the organ of Corti innervation: Barb-ended lines (green) denote signaling that attracts, or is permissive to, innervation. T-ended lines (red) denote signaling that repels, or is nonpermissive to, innervation. IHCs attract/permit, and OHCs repel, innervation by type I afferents. Both IHCs and OHCs attract/permit innervation by type II afferents, but type I afferent innervation supersedes that of type IIs. Type I afferents induce axodendritic innervation by efferents (EF), whereas type II afferents innervation is required to establish and maintain axosomatic efferent innervation on the hair cell.

of MOC efferent innervation in the wild type) (Fig. 8, B and C). Second, when an oc-IHC is innervated by a type II (instead of type I) afferent, then the MOC efferent terminates axosomatically on the IHC (Fig. 8B). Third, although all oc-IHCs that are not innervated by type I afferents are initially (at P10) innervated by type II afferents, about two-thirds of these collateral innervations are lost with time, and this loss is accompanied by the loss of axosomatic efferent innervation (Fig. 8C). Hence, type I afferent innervation implies axodendritic MOC termination, type II afferent innervation implies axosomatic MOC termination, and lack of afferent innervation implies no MOC termination at all.

Efferent and afferent innervation co-occur

We observed a correlation between whether an oc-IHC was innervated by an afferent fiber and whether it also received efferent innervation. We propose that afferent innervation determines efferent fiber termination and that loss of afferent innervation may lead to the loss of efferent termination at an oc-IHC. In principle, this could also be explained the other way around, with loss of efferent innervation leading to a withdrawal of afferent fibers from oc-IHCs. However, we can rule this out because (i) type I afferents still innervate oc-IHCs in explant cochlear cultures established before the arrival of the efferents (in other words, type I afferent innervation of oc-IHCs is independent of efferents (fig. S7); (ii) it has been shown that in explant cultures set up at P0, despite lacking efferent innervation, OHCs display normal ribbon synapses with presumed type II fibers (*45*, *46*); and (iii) surgical de-efferentiation in neonatal cats, at a time when most efferents have not yet entered the outer compartment, does not alter the innervation of OHCs by type II afferents, even 6 to 11 months after surgery (*58*). This implies that the establishment, and certainly the maintenance, of type I and type II contacts is not dependent on efferent contacts. We therefore conclude that the type of afferent innervation (I, II, or none) received by an oc-IHC determines whether and how the MOC efferents will terminate (axodendritically, axosomatically, or not at all, respectively).

We have found that innervation of oc-IHCs by type I afferents is dependent on the presence or absence of an interposed OHC and that when type I afferents innervate, efferents terminate axodendritically, whereas when type I afferents do not innervate and type II afferents do, efferents terminate axosomatically. Intriguingly, mice that lack the Cav1.3 channel have reduced afferent innervation of IHCs. In this mouse model, afferent contacts are normally established but

are subsequently lost over time (with a loss of type I afferent dendrites and soma). This is accompanied by a reduction of axodendritic LOC contacts and a retention for a longer period of time of MOC axosomatic termination on IHCs (*63*). Our data are consistent with this in that we also find a correlation between type I afferent to IHC contact and axodendritic afferent termination, and of lack of it with axosomatic efferent termination. Although we have shown that oc-IHCs are physiologically equivalent to IHCs with respect to K-currents and lack of electromotility, how differential innervation might contribute to other hair cell biophysical properties (or vice versa) remains to be determined.

MATERIALS AND METHODS

Animals

All animal care and procedures were in strict accordance with the Guide for the Care and Use of Laboratory Animals published by the National Institutes of Health and were approved by Northwestern University's Institutional Animal Care and Use Committee (Animal Study Protocol IS00006235). The floxed *Insm1* mouse allele [generated as described in (*40*)] was bred in the C57BL/6 J background. The Atoh1-Cre knock-in mouse line (*17*) was bred from a mixed background of CD1 and C57BL/6. The Gfi1-Cre knock-in mouse line (*52*) was bred from a C57BL/6 background. The Peripherin-EGFP mouse line (*64*) was provided by E. Yamoah. Similar numbers of male and female animals were used for all analyses. Tests were performed with randomly selected littermate control mice (either $Insm1^{F/F}$ or $Atoh1^{Cre/+}$; $Insm1^{F/+}$, which behaved comparably in all experiments described here).

Immunohistochemistry

Animals from P0, P7, and P10 were deeply anesthetized with isoflurane and decapitated. Older animals (from P15 to P30) were deeply anesthetized with ketamine and intracardially perfused with 4% Paraformaldehyde (PFA) in phosphate-buffered saline (PBS). Cochlea were then removed and postfixed in 4% PFA for 2 hours at room temperature (P0, P7, P10, and P15) or overnight at 4°C (P21 to P30). Tissues were washed with PBS and incubated with 10% EDTA (pH 7.4) for 24 to 72 hours depending on age to decalcify the temporal bones. After rinsing with PBS, cochleae were dissected into four turns (an apical turn, two medial turns, and a basal turn) for whole-mount processing. For all staining, unless otherwise noted, equivalent middle (second and third) turns were selected from control and mutant cochlea. The cochlea turns were incubated with 30% sucrose for 20 min, permeabilized by freeze-thaw (−80°C for 7 min followed by a thaw at room temperature for 10 min), and then washed with 1× PBS for 20 min. The turns were incubated with blocking solution [10% normal donkey serum in PBS/T (PBS with 1% TX-100)] for 1 hour at room temperature. Primary antibodies were added to the cochlea turns in blocking solution, and samples were incubated overnight at 37°C [modified from (*28*); see below for antibodies used in this study]. Tissue was then washed three times in 1× PBS and incubated with Alexa- or DyLight-conjugated secondary antibodies for 2 to 3 hours at 37°C. Cochlea turns were washed with 1× PBS and nuclei counterstained with 4′,6-diamidino-2-phenylindole in 1× PBS for 15 min before a final wash and mounting in Prolong Gold antifade mounting medium. For GLAST immunolabeling, tissues were postfixed in 4% PFA in PBS for 30 min and incubated in 10 mM sodium citrate and 0.25% TX-100 (pH 6) for 20 min at 92°C. Tissues were then cooled to room temperature and washed in 1× PBS before incubation in blocking solution for 1 hour at room temperature, followed by primary and secondary antibody incubation as above.

Antibodies used in this study were as follows: Rabbit anti-EAAT1 (GLAST) at 1:100 (catalog no. ab416, Abcam) to label IBCs and IPhCs; rabbit anti-p75 at 1:100 (catalog no. AB1554, Millipore) to label IPCs; rabbit anti-Prox1 at 1:500 (catalog no. AB5475, Millipore) to label nuclei of IPCs, OPCs, and DCs; anti–α-tubulin 1:400 (catalog no. T6199, Sigma-Aldrich) to label IPCs, OPCs, and DCs; rabbit anti-calretinin (Calb2) at 1:100 (catalog no. 7697, Swant) to label type I afferent fibers and type I afferents; mouse anti-CtBP2 at 1:100 (catalog no. 612044, BD Transduction) and mouse anti-GluR2/3 at 1:2000 (catalog no. MAB397, MilliporeSigma) to label presynaptic ribbons and postsynaptic receptors, respectively; goat anti-vAChT at 1:250 (catalog no. ABN100, MilliporeSigma) to label efferent terminals; rabbit anti-TH at 1:500 (catalog no. 657012, MilliporeSigma) to label a subset of LOCs; rabbit anti–Na^+/K^+-ATPase α3 at 1:100 (catalog no. 06-172-1, MilliporeSigma) to label MOCs; mouse anti-CGRP at 1:100 (catalog no. 200-301-D15, Rockland) to label all efferent fibers and terminals; goat anti-parvalbumin at 1:2000 (catalog no. PVG213, Swant); mouse anti-parvalbumin at 1:250 (catalog no. MAB1572, MilliporeSigma) to label type II fibers and their collateral projections; rabbit anti-KCNQ4 at 1:500 [a gift from B. Kachar (*65*)] to label the KCNQ4 potassium channel expressed in OHCs; rabbit anti-BK at 1:500 (catalog no. AOC-021, Alomone Labs) to label the BK potassium channel expressed in IHCs; mouse anti-neurofilament 200-kDa clone RT97 at 1:100 (catalog no. MAB5262, Millipore), rabbit anti-peripherin at 1:200 (catalog no. AB1530), and chicken anti-GFP at 1:500 (catalog no. ab13970, Abcam) to label type II afferent fibers.

Image acquisition and analysis

Images were acquired using either a Yokogawa CSU-W1 spinning disk on a Nikon Ti2 microscope with a Hamamatsu Flash 4 V3 camera operated by NIS-Elements or a Nikon A1 confocal microscope. For the spinning disk, an Apo TIRF 100× Oil DIC objective was used with a numerical aperture of 1.49 using a step size of 0.2 μm, image size of 2048 × 2044, and pixel size of 0.06 μm per pixel. For imaging cultures, a Plan Apo λ 60× Oil objective with a numerical aperture of 1.4 was used with a step size of 0.3 μm, image size of 1024 × 1024, and pixel size of 0.09 μm per pixel. Exposure times were set to ensure high signal to noise and no saturation in the image. For the A1, a Plan Apo λ 100× Oil objective was used with a numerical aperture of 1.45 using a step size of 0.3 μm, image size of 1024 × 1024, and pixel size of 0.09 μm per pixel. Gain and offset adjusting were performed to ensure that no saturated or undersaturated pixels were present.

Images were processed and three-dimensional (3D) renderings generated using NIS-Elements and Imaris, and analysis performed with either Imaris or ImageJ (as described below). We did not see a difference in the number of fibers innervating oc-IHCs (fig. S8A) nor in the number of Ctbp2-positive puncta present in oc-IHCs depending on location along the cochlea (from the apex to the base) (fig. S8B). However, unless otherwise noted, our analysis was performed with middle (second and third) cochlear turns.

Counting fibers

Imaris was used to create a detailed surface rendering of Calb2- and parvalbumin-labeled afferent fibers. *Z*-stacks generated from confocal microscopy were transferred to Imaris where they were displayed as

3D volume rendering for all channels. We used the create surface tool to make a solid surface that best matched the structure of the neuronal fiber (so as to include as much of the neuron as possible while excluding any background) as has been previously described in (*66*). The markers that we use to label type I and type II fibers (e.g., Calb2 and parvalbumin) also label both IHCs and oc-IHCs (with the hair cells labeling more intensely than the fibers), resulting in a huge intensity range within our images. The automatic thresholding judgment made by Imaris fails to capture some of the dimmer fibers. Therefore, the threshold was manually reduced to ensure that all fibers were selected for analysis. Any artifacts (such as staining outside of the region where neurons track in the organ of Corti) were filtered out on the basis of size, sphericity, and position in the *z*-stack. For parvalbumin-labeled fibers, as we were only interested in the labeled fibers associated with the most lateral row (row 3), we filtered out any staining outside of this boundary.

Counting ribbons

The ImageJ plugin, Cell Counter, was used to count ribbons and GluR2/3-positive puncta from 3D-rendered images converted into a single stack (maximum projected intensity). Ribbons or GluR2/3-positive puncta were counted for around 10 cells per image, and then the average number of ribbons was averaged per cell. Numbers generated using this method were comparable to counts achieved when counting ribbons using a wide-field microscope.

Counting vAChT boutons

vAChT staining was assessed in two different ways. For images presented in Fig. 5, counting was performed using a wide-field microscope, and cells were scored as to whether they received a large vAChT-positive efferent terminal or, alternatively, many, dispersed vAChT-positive efferent terminals. In Fig. 7 and fig. S4, Imaris was used to generate a detailed surface rendering of vAChT-positive efferent terminals (as described above, with the exception that the automatic thresholding judgment calculated by Imaris was not manually adjusted). The volume of each vAChT-positive terminal associated with an individual cell was then measured using the Imaris Volume Statistics Toolbar.

Determining distance of oc-IHCs from IHCs

Imaris surface rendering of Calb2-labeled fibers and hair cells was performed as described above. Imaris was then used to calculate the distance between the IHC row and oc-IHCs. Using the measurement tool in Imaris, measurement points were placed centrally on an oc-IHC nucleus and centrally on the nucleus of the nearest IHC in the volume-rendered image.

Whole-cell patch-clamp recording

OHCs and oc-IHCs were obtained by gentle pipetting of excised apical turns from adult control or *Insm1* cKO cochleae in the presence of collagenase (1 mg/ml). This procedure left cells in HC/supporting cell clusters, which were further disrupted by centrifugation at 1000*g* for 3 s. After centrifugation, all IHCs were isolated, while OHCs and oc-IHCs remained attached to adjacent OHCs/supporting cells, thus facilitating identification of morphologically similar IHCs and oc-IHCs. IHCs for recording were collected in separate experiments with harsh pipetting without subsequent centrifugation. Recording pipettes were pulled from borosilicate glass to achieve initial bath resistances averaging 3 to 4 megaohms. Recording pipettes were filled with an intracellular solution containing 140 mM KCl, 2 mM $MgCl_2$, 10 mM EGTA, and 10 mM Hepes (pH 7.3). Cells were bathed in Hanks' balanced salt solution (HBSS) (14025, Thermo Fisher Scientific). Pipette offset current was zeroed immediately before the pipette tip contacted the cell membrane. After establishing the whole-cell configuration, the membrane potential was held at −80 mV and the intracellular pressure kept at 0 mmHg (relative to the atmospheric pressure). Command voltages (V_c) were constant step functions of 150-ms duration (from −140 to +80 mV, 10-mV step). Current data were collected by jClamp (SciSoft Company). For cell membrane electric capacitance (C_m) measurement, the electric current response to a sinusoidal V_c (2.5 Hz, 120- to 150-mV amplitude), superimposed with two higher-frequency stimuli (390.6 and 781.2 Hz, 10-mV amplitude), was recorded. C_m was determined by a fast Fourier transform–based admittance analysis (*67*). Since a large membrane electric conductance interferes with C_m measurement, we determined C_m only in low-voltage ranges where the membrane conductance was kept low. All whole-cell recordings were conducted at room temperature using the Axopatch 200B amplifier (Molecular Devices) with a 10-kHz low-pass filter. The V_c values were corrected for the voltage drop due to the series resistance but not for liquid junction potential that was estimated to be ~4 mV.

Explant cultures

For explant cultures, cochleae were isolated from $Atoh1^{Cre/+;}$ $Insm1^{F/F}$ mice shortly after birth (P2). For each sample, the cochlea roof and any excess connective tissue was removed to expose the sensory epithelium [described in (*68*)], which was then transferred to a plastic culture dish containing fresh culture medium [Dulbecco's modified Eagle's medium supplemented with 10% fetal bovine serum, and ampicillin (50 μg/ml)]. The explants were cultured for 6 days at 37°C with 5% CO_2, with fresh culture medium added after 72 hours (to ensure that the explants had adhered well to the culture dish). Following the culture period, the explants were fixed in 4% PFA in PBS for 30 min at room temperature and then processed for immunostaining and confocal microscopy as described above.

FM1-43 uptake

Cochleae were isolated from $Atoh1^{Cre/+;}$ $Insm1^{F/F}$ at P5 and explants set up as described above. After 6 days in vitro, explants were washed in HBSS (14025076, Thermo Fisher Scientific). Once in wash, a 10 μM FM1-43 (T3163, Thermo Fisher Scientific) working solution was prepared in HBSS. The HBSS wash was removed, and the FM1-43/HBSS solution was added and allowed to sit for 20 s. Cultures were then washed three times in HBSS and immediately examined for fluorescence with a Nikon E600 upright fluorescence microscope [first with a Plan Apo 10× lens (with a numerical aperture of 0.45) to locate the tissue and then with a Fluor 40× immersion lens (with a numerical aperture of 0.8 W)]. Images were captured using a Nikon DS-Ri2 Color complementary metal-oxide semiconductor camera. Cultures were then fixed in 4% PFA in PBS for 30 min at room temperature and processed for immunostaining and confocal microscopy, as described above, to label the oc-IHCs.

Statistical analysis

Analyses were performed with Prism 9. A D'Agostino-Pearson normality test was first performed on data. If data passed this test, then a *t* test or analysis of variance (ANOVA) was performed where appropriate (paired versus multiple datasets, respectively). Welch's correction was reported for tests carried out on multiple datasets. Alternatively, if the data were determined to be non-Gaussian by the

D'Agostino-Pearson test, then a Mann-Whitney test was used on paired data. For multiple comparisons, Dunn's multiple comparison test was performed following a Kruskal-Wallis test. The α level for all tests was 0.05. The minimum number of samples needed to have sufficient statistical power to detect differences in innervation of oc-IHCs versus OHCs was determined to be 4, using an α of 0.05, β of 0.2, and power of 0.8. Power calculations were not explicitly performed before each experiment; however sample sizes were selected according to those routinely used in the field. For transparency, *n* values used throughout the study are given in each figure legend.

SUPPLEMENTARY MATERIALS

Supplementary material for this article is available at http://advances.sciencemag.org/cgi/content/full/7/4/eabd8637/DC1

View/request a protocol for this paper from *Bio-protocol*.

REFERENCES AND NOTES

1. H. Spoendlin, Anatomy of cochlear innervation. *Am. J. Otolaryngol.* **6**, 453–467 (1985).
2. P. Dallos, Neurobiology of cochlear hair cells, in *Auditory Physiology and Perception*, Y. Cazals K. Horner L. Demany, Eds. (Elsevier, 1992), pp. 3–17.
3. J. Zheng, W. Shen, D. Z. He, K. B. Long, L. D. Madison, P. Dallos, Prestin is the motor protein of cochlear outer hair cells. *Nature* **405**, 149–155 (2000).
4. M. C. Liberman, J. Gao, D. Z. Z. He, X. Wu, S. Jia, J. Zuo, Prestin is required for electromotility of the outer hair cell and for the cochlear amplifier. *Nature* **419**, 300–304 (2002).
5. H. Liu, J. L. Pecka, Q. Zhang, G. A. Soukup, K. W. Beisel, D. Z. Z. He, Characterization of transcriptomes of cochlear inner and outer hair cells. *J. Neurosci.* **34**, 11085–11095 (2014).
6. J. Waldhaus, R. Durruthy-Durruthy, S. Heller, Quantitative high-resolution cellular map of the organ of Corti. *Cell Rep.* **11**, 1385–1399 (2015).
7. J. C. Burns, M. C. Kelly, M. Hoa, R. J. Morell, M. W. Kelley, Single-cell RNA-seq resolves cellular complexity in sensory organs from the neonatal inner ear. *Nat. Commun.* **6**, 8557 (2015).
8. M. W. Kelley, E. C. Driver, C. Puligilla, Regulation of cell fate and patterning in the developing mammalian cochlea. *Curr. Opin. Otolaryngol. Head Neck Surg.* **17**, 381–387 (2009).
9. A. C. Meyer, T. Frank, D. Khimich, G. Hoch, D. Riedel, N. M. Chapochnikov, Y. M. Yarin, B. Harke, S. W. Hell, A. Egner, T. Moser, Tuning of synapse number, structure and function in the cochlea. *Nat. Neurosci.* **12**, 444–453 (2009).
10. A. V. Bulankina, T. Moser, Neural circuit development in the mammalian cochlea. *Physiology (Bethesda)* **27**, 100–112 (2012).
11. A. M. Berglund, D. K. Ryugo, Hair cell innervation by spiral ganglion neurons in the mouse. *J. Comp. Neurol.* **255**, 560–570 (1987).
12. W. B. Warr, Organization of olivocochlear efferent systems in mammals, in *The Mammalian Auditory Pathway: Neuroanatomy*, D. B. Webster, A. N. Popper, R. R. Fay, Eds. (Springer New York, 1992), pp. 410–448.
13. D. D. Simmons, Development of the inner ear efferent system across vertebrate species. *J. Neurobiol.* **53**, 228–250 (2002).
14. A. B. Elgoyhen, E. Katz, The efferent medial olivocochlear-hair cell synapse. *J. Physiol. Paris* **106**, 47–56 (2012).
15. M. M. Frank, L. V. Goodrich, Talking back: Development of the olivocochlear efferent system. *Wiley Interdiscip. Rev. Dev. Biol.* **7**, e324 (2018).
16. B. R. Shrestha, L. V. Goodrich, Wiring the cochlea for sound perception, in *The Oxford Handbook of the Auditory Brainstem*, K. Kandler, Ed. (Oxford Univ. Press, 2019), Chapter 1, pp. 1-40.
17. H. Yang, X. Xie, M. Deng, X. Chen, L. Gan, Generation and characterization of Atoh1-Cre knock-in mouse line. *Genesis* **48**, 407–413 (2010).
18. Y.-S. Lee, F. Liu, N. Segil, A morphogenetic wave of p27Kip1 transcription directs cell cycle exit during organ of Corti development. *Development* **133**, 2817–2826 (2006).
19. P. Chen, J. E. Johnson, H. Y. Zoghbi, N. Segil, The role of Math1 in inner ear development: Uncoupling the establishment of the sensory primordium from hair cell fate determination. *Development* **129**, 2495–2505 (2002).
20. E. J. Koundakjian, J. L. Appler, L. V. Goodrich, Auditory neurons make stereotyped wiring decisions before maturation of their targets. *J. Neurosci.* **27**, 14078–14088 (2007).
21. W. Y. Kim, B. Fritzsch, A. Serls, L. A. Bakel, E. J. Huang, L. F. Reichardt, D. S. Barth, J. E. Lee, NeuroD-null mice are deaf due to a severe loss of the inner ear sensory neurons during development. *Development* **128**, 417–426 (2001).
22. T. M. Coate, S. Raft, X. Zhao, A. K. Ryan, E. B. Crenshaw, M. W. Kelley, Otic mesenchyme cells regulate spiral ganglion axon fasciculation through a Pou3f4/EphA4 signaling pathway. *Neuron* **73**, 49–63 (2012).
23. T. M. Coate, N. A. Spita, K. D. Zhang, K. T. Isgrig, M. W. Kelley, Neuropilin-2/Semaphorin-3F-mediated repulsion promotes inner hair cell innervation by spiral ganglion neurons. *eLife* **4**, (2015).
24. L.-C. Huang, P. R. Thorne, G. D. Housley, J. M. Montgomery, Spatiotemporal definition of neurite outgrowth, refinement and retraction in the developing mouse cochlea. *Development* **134**, 2925–2933 (2007).
25. N. R. Druckenbrod, L. V. Goodrich, Sequential retraction segregates SGN processes during target selection in the cochlea. *J. Neurosci.* **35**, 16221–16235 (2015).
26. P. Vyas, J. S. Wu, A. Zimmerman, P. Fuchs, E. Glowatzki, Tyrosine hydroxylase expression in type II cochlear afferents in mice. *J. Assoc. Res. Otolaryngol.* **18**, 139–151 (2017).
27. P. Vyas, J. S. Wu, A. Jimenez, E. Glowatzki, P. A. Fuchs, Characterization of transgenic mouse lines for labeling type I and type II afferent neurons in the cochlea. *Sci. Rep.* **9**, 5549 (2019).
28. S. Maison, L. D. Liberman, M. C. Liberman, Type II cochlear ganglion neurons do not drive the olivocochlear reflex: Re-examination of the cochlear phenotype in peripherin knock-out mice. *Eneuro* **3**, ENEURO.0207–ENEU16.2016 (2016).
29. J. Defourny, A.-L. Poirrier, F. Lallemend, S. Mateo Sánchez, J. Neef, P. Vanderhaeghen, E. Soriano, C. Peuckert, K. Kullander, B. Fritzsch, L. Nguyen, G. Moonen, T. Moser, B. Malgrange, Ephrin-A5/EphA4 signalling controls specific afferent targeting to cochlear hair cells. *Nat. Commun.* **4**, 1438 (2013).
30. A. I. Lyuksyutova, C.-C. Lu, N. Milanesio, L. A. King, N. Guo, Y. Wang, J. Nathans, M. Tessier-Lavigne, Y. Zou, Anterior-posterior guidance of commissural axons by Wnt-frizzled signaling. *Science* **302**, 1984–1988 (2003).
31. K. Onishi, B. Shafer, C. Lo, F. Tissir, A. M. Goffinet, Y. Zou, Antagonistic functions of Dishevelleds regulate Frizzled3 endocytosis via filopodia tips in Wnt-mediated growth cone guidance. *J. Neurosci.* **33**, 19071–19085 (2013).
32. B. Shafer, K. Onishi, C. Lo, G. Colakoglu, Y. Zou, Vangl2 promotes Wnt/planar cell polarity-like signaling by antagonizing Dvl1-mediated feedback inhibition in growth cone guidance. *Dev. Cell* **20**, 177–191 (2011).
33. S. R. Ghimire, M. R. Deans, *Frizzled3* and *Frizzled6* cooperate with *Vangl2* to direct cochlear innervation by type II spiral ganglion neurons. *J. Neurosci.* **39**, 8013–8023 (2019).
34. S. M. Echteler, Developmental segregation in the afferent projections to mammalian auditory hair cells. *Proc. Natl. Acad. Sci. U.S.A.* **89**, 6324–6327 (1992).
35. A. L. Bergeron, A. Schrader, D. Yang, A. A. Osman, D. D. Simmons, The final stage of cholinergic differentiation occurs below inner hair cells during development of the rodent cochlea. *J. Assoc. Res. Otolaryngol.* **6**, 401–415 (2005).
36. A. Shnerson, C. Devigne, R. Pujol, Age-related changes in the C57BL/6J mouse cochlea. II. Ultrastructural findings. *Dev. Brain Res.* **2**, 77–88 (1981).
37. G. Kearney, J. Z. de San Martín, L. G. Vattino, A. B. Elgoyhen, C. Wedemeyer, E. Katz, Developmental synaptic changes at the transient olivocochlear-inner hair cell synapse. *J. Neurosci.* **39**, 3360–3375 (2019).
38. R. Pujol, E. Carlier, C. Devigne, Different patterns of cochlear innervation during the development of the kitten. *J. Comp. Neurol.* **177**, 529–535 (1978).
39. Q. Ma, D. J. Anderson, B. Fritzsch, Neurogenin 1 null mutant ears develop fewer, morphologically normal hair cells in smaller sensory epithelia devoid of innervation. *J. Assoc. Res. Otolaryngol.* **1**, 129–143 (2000).
40. T. Wiwatpanit, S. M. Lorenzen, J. A. Cantú, C. Z. Foo, A. K. Hogan, F. Márquez, J. C. Clancy, M. J. Schipma, M. A. Cheatham, A. Duggan, J. García-Añoveros, Trans-differentiation of outer hair cells into inner hair cells in the absence of INSM1. *Nature* **563**, 691–695 (2018).
41. S. M. Lorenzen, A. Duggan, A. B. Osipovich, M. A. Magnuson, J. García-Añoveros, Insm1 promotes neurogenic proliferation in delaminated otic progenitors. *Mech. Dev.* **138**, 233–245 (2015).
42. B. R. Shrestha, C. Chia, L. Wu, S. G. Kujawa, M. C. Liberman, L. V. Goodrich, Sensory neuron diversity in the inner ear is shaped by activity. *Cell* **174**, 1229–1246.e17 (2018).
43. C. Petitpré, H. Wu, A. Sharma, A. Tokarska, P. Fontanet, Y. Wang, F. Helmbacher, K. Yackle, G. Silberberg, S. Hadjab, F. Lallemend, Neuronal heterogeneity and stereotyped connectivity in the auditory afferent system. *Nat. Commun.* **9**, 3691 (2018).
44. S. Sun, T. Babola, G. Pregernig, K. S. So, M. Nguyen, S.-S. M. Su, A. T. Palermo, D. E. Bergles, J. C. Burns, U. Müller, Hair cell mechanotransduction regulates spontaneous activity and spiral ganglion subtype specification in the auditory system. *Cell* **174**, 1247–1263.e15 (2018).
45. H. M. Sobkowicz, J. E. Rose, G. L. Scott, C. V. Levenick, Distribution of synaptic ribbons in the developing organ of Corti. *J. Neurocytol.* **15**, 693–714 (1986).
46. H. M. Sobkowicz, J. E. Rose, G. E. Scott, S. M. Slapnick, Ribbon synapses in the developing intact and cultured organ of Corti in the mouse. *J. Neurosci.* **2**, 942–957 (1982).
47. L. D. Liberman, M. C. Liberman, Postnatal maturation of auditory-nerve heterogeneity, as seen in spatial gradients of synapse morphology in the inner hair cell area. *Hear. Res.* **339**, 12–22 (2016).

48. F. A. Thiers, J. B. Nadol, M. C. Liberman, Reciprocal synapses between outer hair cells and their afferent terminals: Evidence for a local neural network in the mammalian cochlea. *J. Assoc. Res. Otolaryngol.* **9**, 477–489 (2008).
49. M. C. Liberman, L. W. Dodds, S. Pierce, Afferent and efferent innervation of the cat cochlea: Quantitative analysis with light and electron microscopy. *J. Comp. Neurol.* **301**, 443–460 (1990).
50. M. C. Liberman, Morphological differences among radial afferent fibers in the cat cochlea: An electron-microscopic study of serial sections. *Hear. Res.* **3**, 45–63 (1980).
51. N. Y. Kiang, J. M. Rho, C. C. Northrop, M. C. Liberman, D. K. Ryugo, Hair-cell innervation by spiral ganglion cells in adult cats. *Science* **217**, 175–177 (1982).
52. H. Yang, J. Gan, X. Xie, M. Deng, L. Feng, X. Chen, Z. Gao, L. Gan, Gfi1-Cre knock-in mouse line: A tool for inner ear hair cell-specific gene deletion. *Genesis* **48**, 400–406 (2010).
53. K. N. Darrow, E. J. Simons, L. Dodds, M. C. Liberman, Dopaminergic innervation of the mouse inner ear: Evidence for a separate cytochemical group of cochlear efferent fibers. *J. Comp. Neurol.* **498**, 403–414 (2006).
54. W. J. McLean, K. A. Smith, E. Glowatzki, S. J. Pyott, Distribution of the Na,K-ATPase α subunit in the rat spiral ganglion and organ of Corti. *J. Assoc. Res. Otolaryngol.* **10**, 37–49 (2009).
55. S. F. Maison, R. B. Emeson, J. C. Adams, A. E. Luebke, M. C. Liberman, Loss of alpha CGRP reduces sound-evoked activity in the cochlear nerve. *J. Neurophysiol.* **90**, 2941–2949 (2003).
56. R. E. Perkins, D. K. Morest, A study of cochlear innervation patterns in cats and rats with the Golgi method and Nomarkski Optics. *J. Comp. Neurol.* **163**, 129–158 (1975).
57. D. D. Simmons, A transient afferent innervation of outer hair cells in the postnatal cochlea. *Neuroreport* **5**, 1309–1312 (1994).
58. M. C. Liberman, D. F. O'Grady, L. W. Dodds, J. McGee, E. J. Walsh, Afferent innervation of outer and inner hair cells is normal in neonatally de-efferented cats. *J. Comp. Neurol.* **423**, 132–139 (2000).
59. C. Puligilla, F. Feng, K. Ishikawa, S. Bertuzzi, A. Dabdoub, A. J. Griffith, B. Fritzsch, M. W. Kelley, Disruption of fibroblast growth factor receptor 3 signaling results in defects in cellular differentiation, neuronal patterning, and hearing impairment. *Dev. Dyn.* **236**, 1905–1917 (2007).
60. M. M. Mellado Lagarde, B. C. Cox, J. Fang, R. Taylor, A. Forge, J. Zuo, Selective ablation of pillar and Deiters' cells severely affects cochlear postnatal development and hearing in mice. *J. Neurosci.* **33**, 1564–1576 (2013).
61. K. D. Zhang, T. M. Coate, Recent advances in the development and function of type II spiral ganglion neurons in the mammalian inner ear. *Semin. Cell Dev. Biol.* **65**, 80–87 (2017).
62. S. R. Ghimire, E. M. Ratzan, M. R. Deans, A non-autonomous function of the core PCP protein VANGL2 directs peripheral axon turning in the developing cochlea. *Development* **145**, dev159012 (2018).
63. R. M. Nemzou N, A. V. Bulankina, D. Khimich, A. Giese, T. Moser, Synaptic organization in cochlear inner hair cells deficient for the CaV1.3 (alpha1D) subunit of L-type Ca2+ channels. *Neuroscience* **141**, 1849–1860 (2006).
64. S. McLenachan, Y. Goldshmit, K. J. Fowler, L. Voullaire, T. P. Holloway, A. M. Turnley, P. A. Ioannou, J. P. Sarsero, Transgenic mice expressing the Peripherin-EGFP genomic reporter display intrinsic peripheral nervous system fluorescence. *Transgenic Res.* **17**, 1103–1116 (2008).
65. K. W. Beisel, S. M. Rocha-Sanchez, K. A. Morris, L. Nie, F. Feng, B. Kachar, E. N. Yamoah, B. Fritzsch, Differential expression of KCNQ4 in inner hair cells and sensory neurons is the basis of progressive high-frequency hearing loss. *J. Neurosci.* **25**, 9285–9293 (2005).
66. M. J. Fogarty, L. A. Hammond, R. Kanjhan, M. C. Bellingham, P. G. Noakes, A method for the three-dimensional reconstruction of Neurobiotin™-filled neurons and the location of their synaptic inputs. *Front. Neural Circuits* **7**, 153 (2013).
67. J. Santos-Sacchi, S. Kakehata, S. Takahashi, Effects of membrane potential on the voltage dependence of motility-related charge in outer hair cells of the guinea-pig. *J. Physiol. Lond.* **510**, 225–235 (1998).
68. K. D. Haque, A. K. Pandey, M. W. Kelley, C. Puligilla, Culture of embryonic mouse cochlear explants and gene transfer by electroporation. *J. Vis. Exp.* , 52260 (2015).
69. J. R. Meyers, R. B. MacDonald, A. Duggan, D. Lenzi, D. G. Standaert, J. T. Corwin, D. P. Corey, Lighting up the senses: FM1-43 loading of sensory cells through nonselective ion channels. *J. Neurosci.* **23**, 4054–4065 (2003).

Acknowledgments: We thank S. DeVries, D. Whitlon, M.A. Cheatham, and S. Takahashi for helpful feedback and comments on the manuscript. Imaging work was performed at the Northwestern University Center for Advanced Microscopy supported by NCI CCSG P30 CA060553 awarded to the Robert H. Lurie Comprehensive Cancer Center. Spinning disk confocal microscopy was performed on an Andor XDI Revolution microscope purchased through the support of NCRR 1S10 RR031680-01. **Funding:** This study was supported by R01 DC015903 to J.G.-A., R01 DC017482 to K.H., and K01 DC018852 mentored career development award to J.L.W. The content is solely the responsibility of the authors and does not necessarily represent the official views of the National Institutes of Health. **Author contributions:** Conceptualization: J.G.-A. Methodology: J.L.W., J.C.C., Y.Z., K.H., and J.G.-A. Data collection: J.L.W., J.C.C., K.H., Y.Z., and N.Y. Data analysis: J.L.W., K.H., and J.G.-A. Writing: J.L.W. and J.G.-A. Supervision: J.G.-A. **Competing interests:** The authors declare that they have no competing interests. **Data and materials availability:** All data needed for evaluation of the conclusions drawn here are present in the paper and/or the Supplementary Materials. The Insm1-Flox mice can be provided by J.G.-A. pending scientific review and a completed material transfer agreement. Requests for the Insm1-Flox mice should be submitted to J.G.-A.

Submitted 17 July 2020
Accepted 3 December 2020
Published 20 January 2021
10.1126/sciadv.abd8637

Citation: J. L. Webber, J. C. Clancy, Y. Zhou, N. Yraola, K. Homma, J. García-Añoveros, Axodendritic versus axosomatic cochlear efferent termination is determined by afferent type in a hierarchical logic of circuit formation. *Sci. Adv.* **7**, eabd8637 (2021).